SOLAR SATELLITE PROJECT

HARVARD COLLEGE OBSERVATORY

60 GARDEN STREET

CAMBRIDGE, MASS

14

HARVARD COLLEGE OSO-IV
POINTED EXPERIMENT
AN ANALYSIS OF THE
MALFUNCTION DURING
ORBIT 637

BY: R. Dower
N. Hazen
J. Rechavi

Technical Report No. 7
NASA Contract NASw-184

February 1969

TABLE OF CONTENTS

Table of Contents

LIST OF ILLUSTRATIONS

List of Illustrations

LIST OF TABLES

ABSTRACT

The Harvard College Observatory pointed experiment aboard OSO-IV suffered a disabling electronic malfunction after a few weeks of successful scientific operation. This report describes the investigations which were undertaken to evaluate the malfunction. The initial observations are described, and the total available data are then reviewed in detail. This report describes analyses which were undertaken both with the data and with the design information on the instrument. It also includes studies which were performed in the laboratory with the prototype instrument and various sub-assemblies. Conclusions are drawn which strongly implicate the high voltage power supply - particularly the transformer - as the origin of the malfunction. Recommendations are made on how similar problems might be avoided in the future.

1.0 INTRODUCTION

The Harvard College Observatory ultraviolet spectroheliometer instrument was successfully launched as part of the Orbiting Solar Observatory IV on October 18, 1967. On November 29, 1967, after a few weeks of highly successful scientific operation, the telemetered data indicated that a malfunction had taken place in the instrument.

A Quick-Look Data System has been set up at Fort Myers, Florida, station which supplies Harvard experiments with immediate data. The Quick-Look data available to HCO experimenters indicated that the primary current readings for the instrument's high voltage power supply were abnormally high. The power supply was immediately turned off, and attempts made shortly t reafter to eliminate the problem by switching the power supply back on were unsuccessful. No further useful scientific data have been received from the instrument since that time, although considerable additional engineering testing has been accomplished.

Intensive review of the available data took place during the hours and days following the first observation of difficulty. The available data included not only that received from the Fort Myers passes by the Quick-Look System, but also that from the several orbits taken especially from the Santiago and Johannesburg stations. The initial occurrence of difficulty was soon identified in data from orbit 637 which had been taken by the Johannesburg station.

Analysis of the data received after the termination of the UV data made it clear that the malfunction was a progressive one. This was indicated in the data by the presence of two modes which differ from those of normal operation. The two abnormal modes have data characteristics substantially different from one another.

Mode I was characterized by an almost maximum high voltage current (the HCO high voltage current monitor supplies these data), by noise counts, and by false mechanical reference indications.

Mode II also appeared to be characterized by near maximum high voltage current. However, there is no evidence that this mode represents accompanying effects in the instrument.

Subsequent sections of this report will be concerned with the background material on the spacecraft and instrument, the operational aspects of the malfunction, a detailed review of the telemetry data, and analyses of the several aspects and hypotheses of the malfunction. Conclusions are drawn concerning the nature of the malfunction and the difficulties in the high voltage power supply, and recommendations are made toward minimizing the possibility that this kind of failure will recur.

2.0 GENERAL BACKGROUND

2.1 OSO-IV SPACECRAFT

Ozone, molecular oxygen, and other components of the earth's atmosphere absorb the incident solar radiation with wavelength less than 2900Å before it reaches the earth's surface. This prevents ground-based observations of most of the ultraviolet (UV) and x-ray region of the solar spectrum. Suborbital rockets and orbiting satellites provide observation platforms which are not subject to the atmospheric limitation.

The Orbiting Solar Observatory IV (OSO-IV) spacecraft contains nine experiments to investigate solar phenomena primarily in the ultraviolet and x-ray regions. OSO-IV was launched on October 18, 1967. It achieved a nearly circular orbit 547.5 ±2.5 kilometers above the earth's surface at an inclination to the equator of 33°. Further information on the design and experimental complement of OSO-IV can be obtained from the documents listed in the bibliography.

2.2 HCO INSTRUMENT

The Harvard College Observatory (HCO) instrument in the OSO-IV spacecraft is an ultraviolet spectroheliometer designed to gather data on solar radiation in the 300Å-1300Å wavelength range. The instrument operates in either of two modes. In the wavelength-scan mode the instrument points at the center of the sun while its spectrometer scans the spectrum from 300Å to 1300Å once every 30 minutes. From this a plot of the photon count (i.e., intensity) vs. wavelength is obtained.

In the raster mode the spectrometer is positioned at a fixed wavelength and the spacecraft scans the instrument field of view over the solar disc in a raster pattern of forty lines with forty-eight measurements of intensity taken on each line. A spectroheliogram is constructed of data obtained in the raster mode.

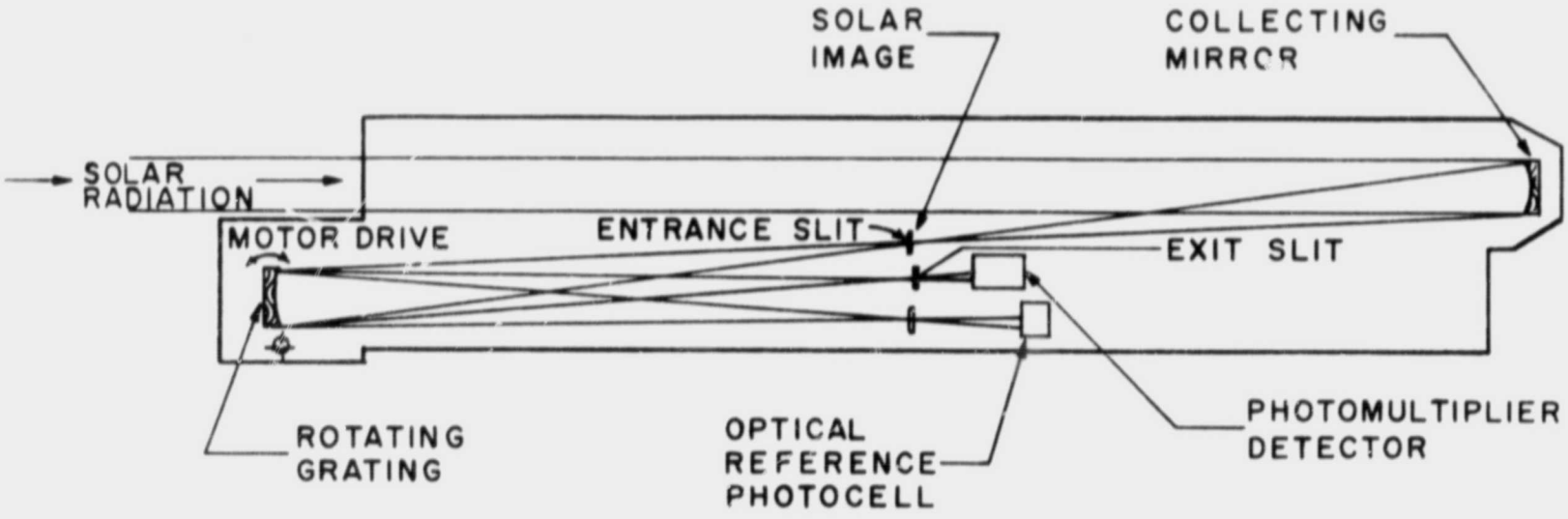

Figure 1.
OPTICAL DIAGRAM OF HARVARD INSTRUMENT

An optical diagram of the HCO instrument is shown in Figure 1. Sunlight enters through the aperture and is reflected by the spherical mirror to form a solar image on the entrance slit. The entrance slit acts as a field stop that allows light from a one arc minute square area of the sun to pass to the diffraction grating. The grating diffracts the incident light into its emission line spectrum. By rotating the grating, successive wavelengths

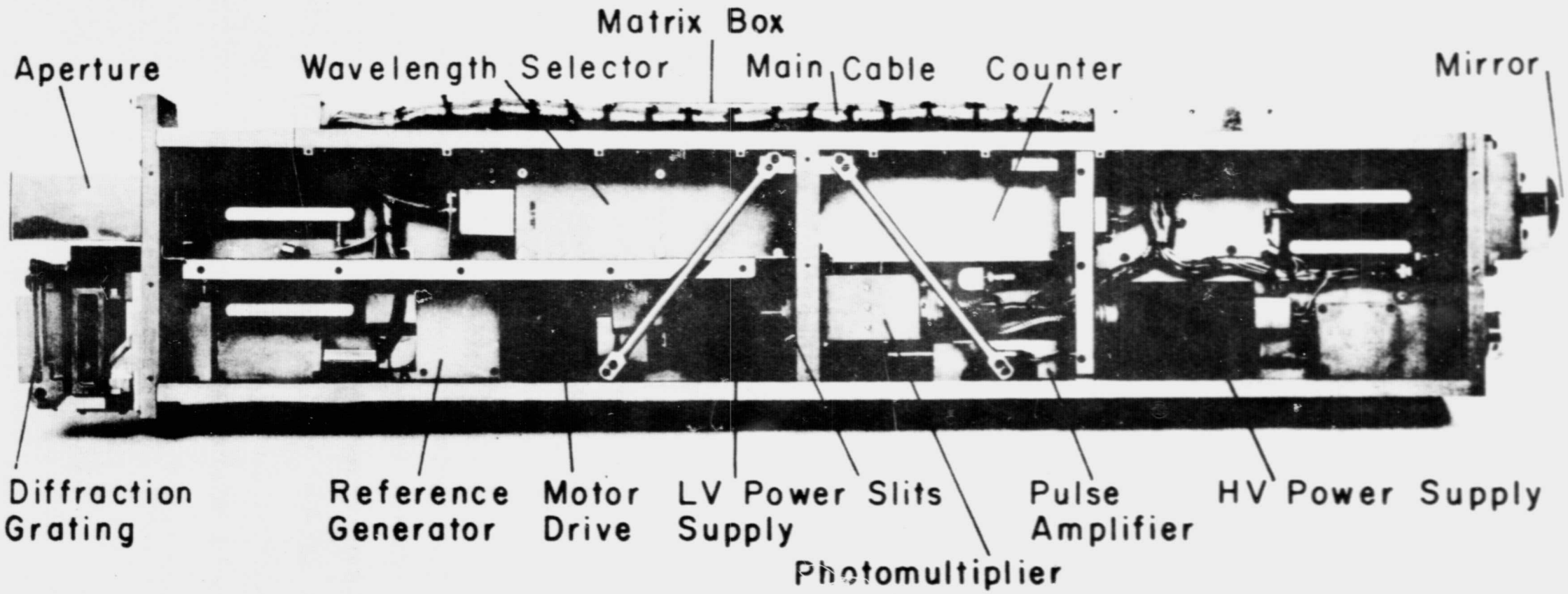

Figure 2 — HARVARD OSO-D INSTRUMENT

are imaged on the exit slit. The combined slit widths give the instrument a spectral resolution such that the intensity of two lines separated by 2.2Å could be measured separately. Ultraviolet photons passing through the exit slit and impinging on the photomultiplier cathode produce current pulses at its anode that are amplified and counted.

The photograph in Figure 2 is labeled to show the positions of various components within the HCO instrument. The working relationships of these components are illustrated in the block diagram of Figure 3. Readers unfamiliar with the HCO instrument may refer to the HCO OSO-D Experiment Handbook (May 1, 1966) for details on the function of the various components. (see bibliography)

2.3 HCO DATA

HCO data are of two general forms: primary signal or "main frame" data, and housekeeping or analog sub-commutated data. In normal operation the primary data from the counter (see Figure 3) indicate the number of current pulses produced by ultraviolet photons impinging on the photomultiplier cathode in a fixed time interval. Also included in each data word is a reference signal indicating when the diffraction grating is in the mechanical (MR) or the optical (OR) reference position. The housekeeping data (from the matrix box) indicate the internal temperature of the instrument, the difference in temperature between the two ends of the instrument, the input current of the high voltage power supply, the position of the diffraction grating, the condition of the readin gate signal, and the signal count rate from the

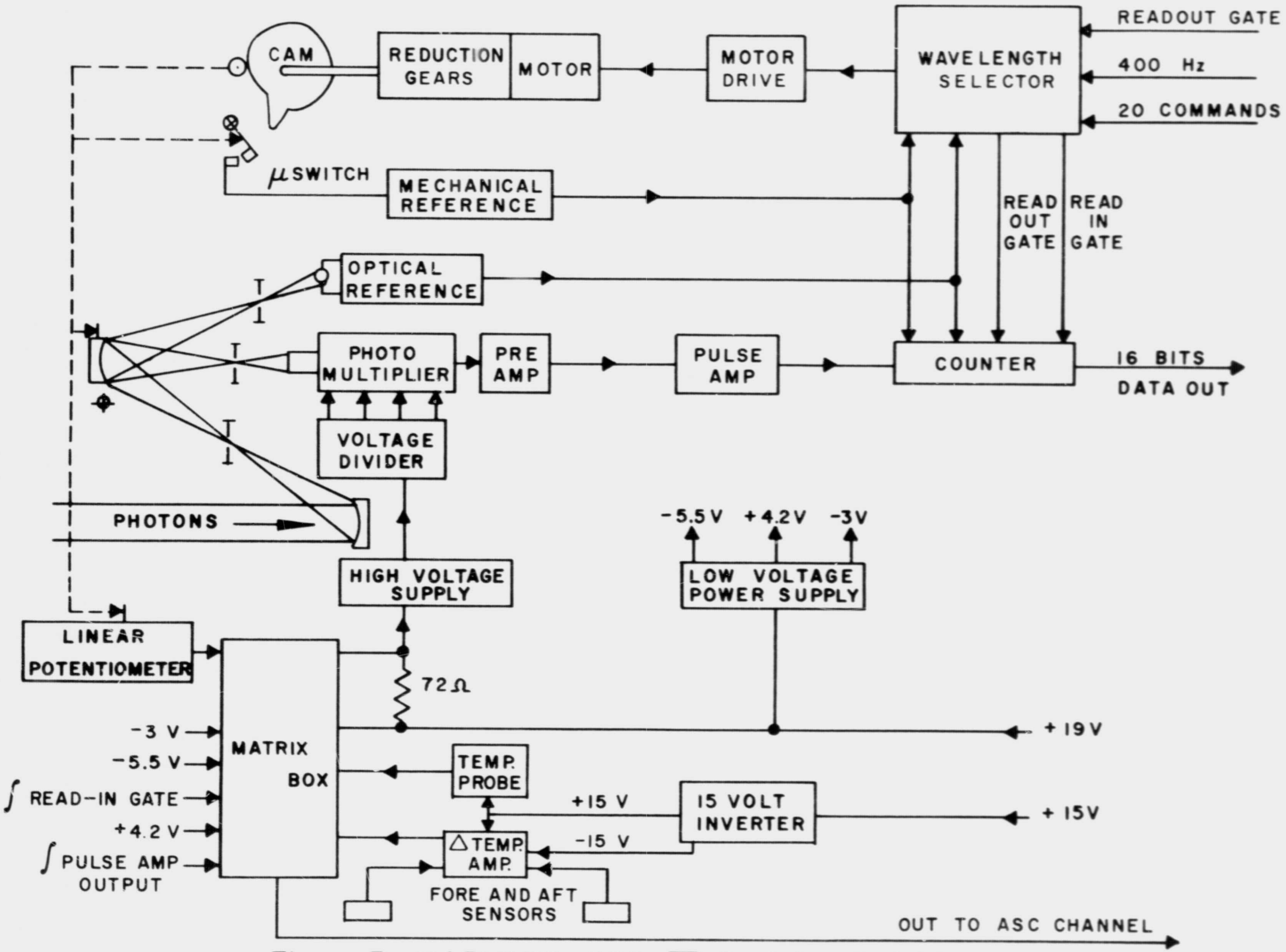

Figure 3- HARVARD OSO-IV BLOCK DIAGRAM

pulse amplifier. See Appendix 1 for further details on the timing, acquisition, and transmission of the HCO data.

3.0 OPERATIONS ASPECTS OF THE TERMINATION PERIOD

3.1 INITIAL EVIDENCE

On November 29, 1967, during orbit 636 the OSO-IV spacecraft made the last of a daily series of passes within range of the Ft. Myers, Florida, STADAN (Satellite Tracking and Data Acquisition Network) station. The next pass within range of the Ft. Myers station occurred 16 hours later during orbit 646 on November 30. During that pass, the satellite played back its tape-recorded data from the previous orbit to Ft. Myers. About 20 minutes after the play-back, Harvard experimenters had received and examined the data from the HCO instrument via the Quick-Look data link. All primary data counts were zeros (abnormal) and the high voltage monitor readings were unusually high and fluctuating. As a result, the instrument's power supplies were commanded off when the spacecraft passed near the Ororal STADAN station in Australia later in the same orbit.

A review of the Quick-Look data from the previous day showed that during orbit 636 the HCO instrument was functioning properly. Harvard experimenters then requested and received additional All Channel data from the Santiago STADAN station in Chile on the following day (December 1). The data were relayed to Ft. Myers through a communication satellite; then printouts were hand carried to HCO. The first pass after orbit 636 within range of the Santiago station occurred two orbits later during orbit 638, but the data showed that by then the counts were already zeros and the high voltage current readings were high and

fluctuating. So the crucial orbit appeared to be 637. An All-Channel printout of the data recorded during orbit 637 at the STADAN station located near Johannesburg, South Africa, was received at HCO on December 13 and contained the desired evidence. Efforts to analyze these data and to simulate malfunction conditions in the prototype HCO instrument commenced immediately.

3.2 SUBSEQUENT OPERATION OF THE INSTRUMENT

Normal data gathering operations of the HCO instrument ended during orbit 637 and the instrument was turned off during orbit 646. Since then many attsmpts have been made to restore it to normal operation or to force a change in mode. The instrument's low voltage power supply was turned on again during orbit 648. In orbit 649 the high voltage power supply (HVPS) was turned on for one minute. Data count noise, spurious Mechanical Reference (MR) bits, and high readings of the input current of the HVPS perished throughout the period. In orbit 650 the HV power supply was turned on for 3.5 minutes. Count noise and false mechanical reference occurred only during the first six seconds of this period. The HV current readings remained high and fluctuating during the entire 3.5 minutes.

Subsequent commands to turn on the HVPS for brief periods during orbits 856, 857, 971 and 1089-1090 yielded the high, fluctuating, analog readings of HVPS current but only zero counts in the main data words. During orbit 1238, five weeks after the end of normal operation, the HVPS was turned on for 2 hours and 50 minutes.

During the first six minutes of that period count noise and false MR bits occurred. The HVPS current readings were high and fluctuating until the supply was turned off.

In the latter part of January the high voltage system was turned on for longer periods of time to see whether any alteration of condition could be induced. On eight occasions it was turned on for a full set of orbital passes (approximately six hours). No alteration was observed.

Starting February 27, 1968, a routine test mode was started involving a trial of the high voltage system for one orbit each day. This continued until mid-May when the last tape recorder failed in the spacecraft. After that, testing was started again in mid-June on a "real time" basis. This involved testing the high voltage system for approximately ten minutes each day during a pass over the Fort Myers STADAN Station. These operations continued through the remainder of the year 1968. During this whole period no unusual effects or reversion of condition were observed. Noise counts were occasionally observed in the data system, but they were unrelated to the high voltage tests. They were particularly pronounced in late April, 1968 and were related to the operation of certain wheel experiments, notably the Lawrence Radiation Laboratory experiment.

Additional orbital experimental testing of the spectrometic system took place during this period, but was unrelated to the high voltage problem.

In particular, the motor drive system was run continuously in the wavelength scan mode from late February through the remainder of the year, with the exception of the one-month period from mid-May to mid-June. In this and all other aspects of routine performance, the instrument appeared to be in good condition throughout the period.

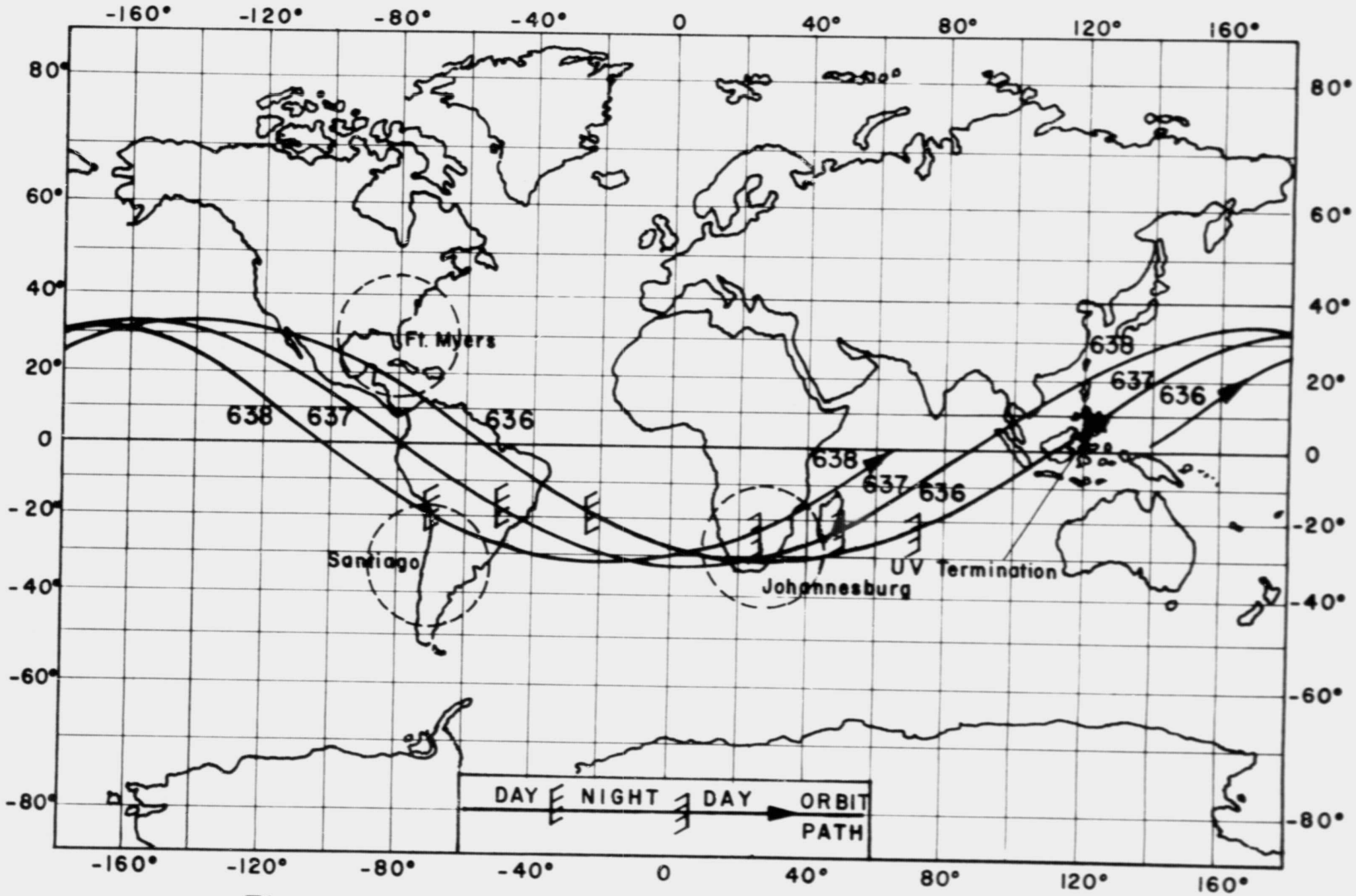

Figure 4— OSO-Ⅳ ORBITS 636-638

4.0 TERMINATION OF UV DATA

4.1 DATA CHARACTERISTICS

As the OSO-IV satellite passed near the Ft. Myers, Florida, STADAN station during orbit 636, the HCO instrument was routinely commanded to step its diffraction grating into position to examine the emission of Ne VIII ions in 770Å radiation. After the data were taken for two complete raster scans of the sun at this wavelength, the satellite entered darkness. Figure 4 illustrates the relevant satellite orbits as reconstructed from data in the Predicted Satellite Map furnished by NASA. While in darkness the satellite tape recorders played back data acquired during orbit 636 to the Johannesburg, South Africa STADAN station. The satellite entered the sunlight again as it headed north toward the equator and began (by definition) orbit 637 as it crossed the equator heading North.

The HCO instrument began raster operation a few seconds after the spacecraft entered sunlight. The HCO data from the first half of this initial raster picture contain very few counts because the instrument takes many seconds to fix on the sun. Also, at satellite dawn and dusk the instrument looks through a maximum amount of the earth's atmosphere, which adsorbs most of the solar ultraviolet radiation. Data for the next four complete raster scans are illustrated in the computer plots of Figures 5A and 5B. The plots on the left indicate UV intensity by the density of ink on the page. The plots on the right

MAX. INTENSITY = 8850

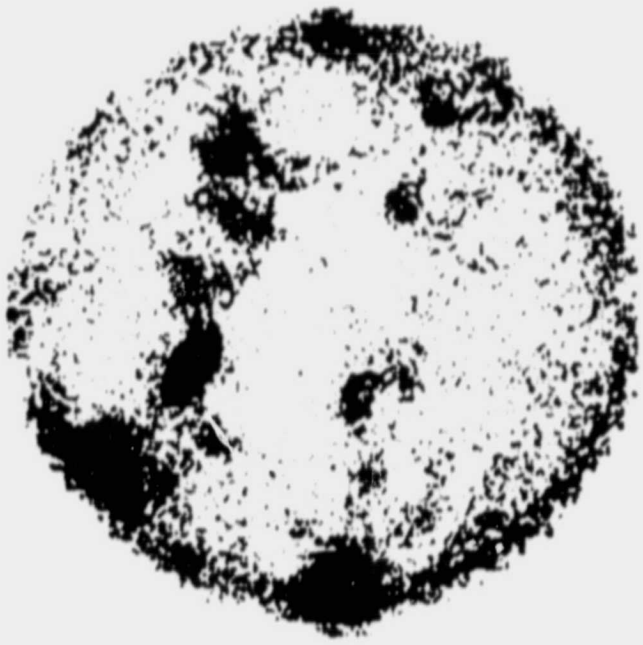

MAX. INTENSITY = 8850

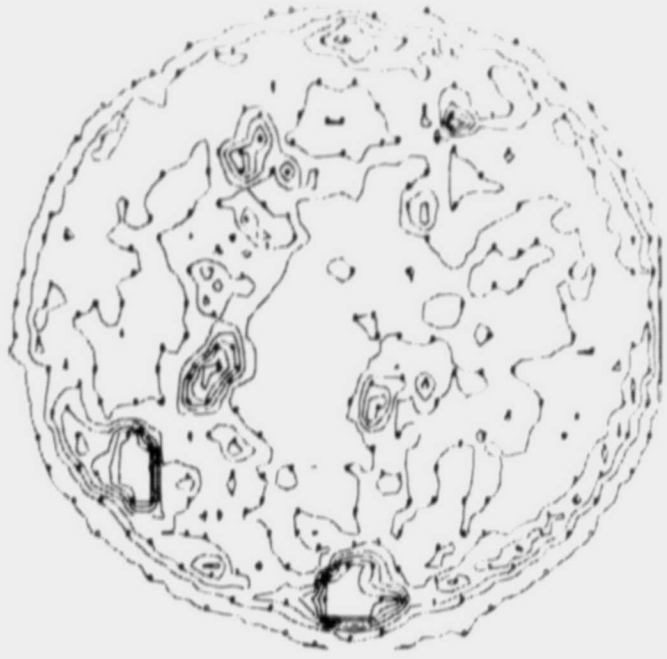

RASTER 2

RASTER 3

MAX. INTENSITY = 6950

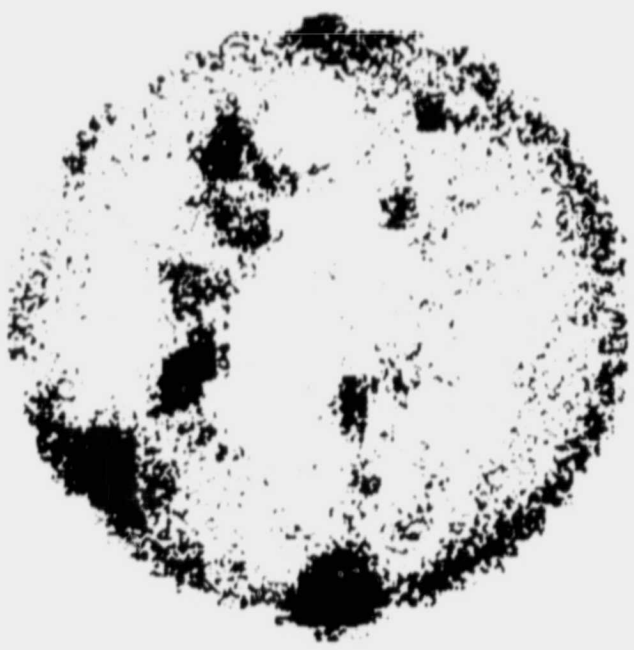

MAX. INTENSITY = 6950

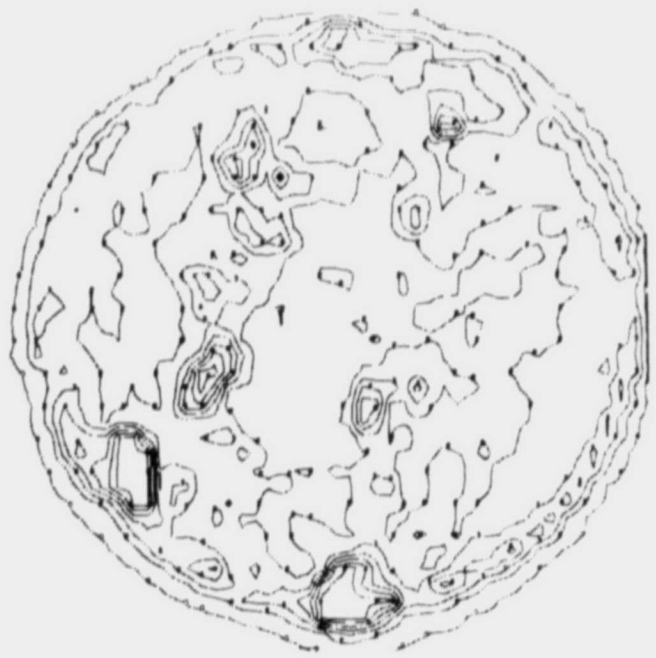

Figure 5A
RASTER PLOTS BEFORE UV
TERMINATION
NE VIII

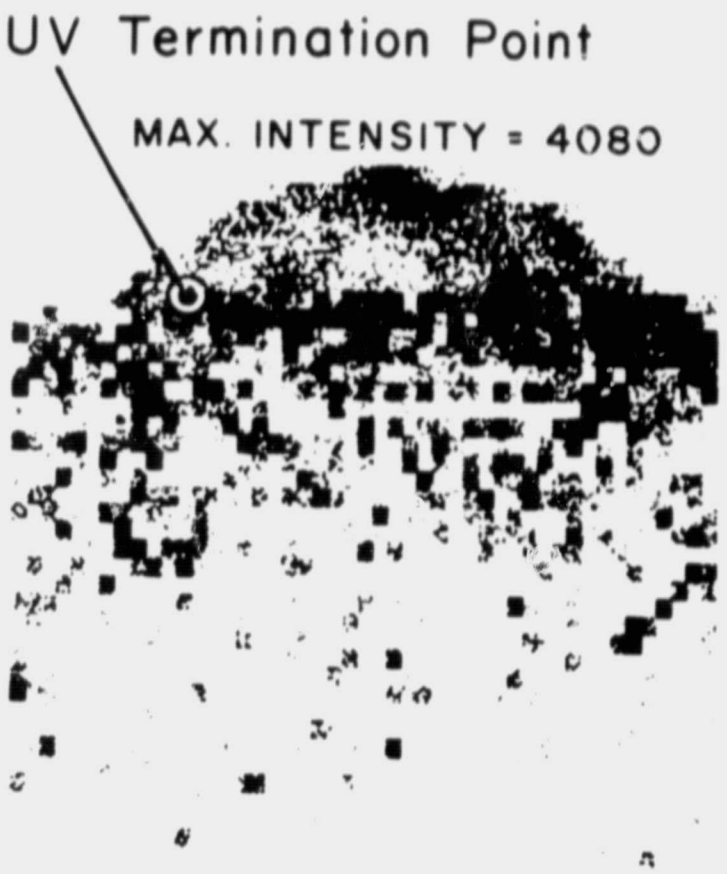

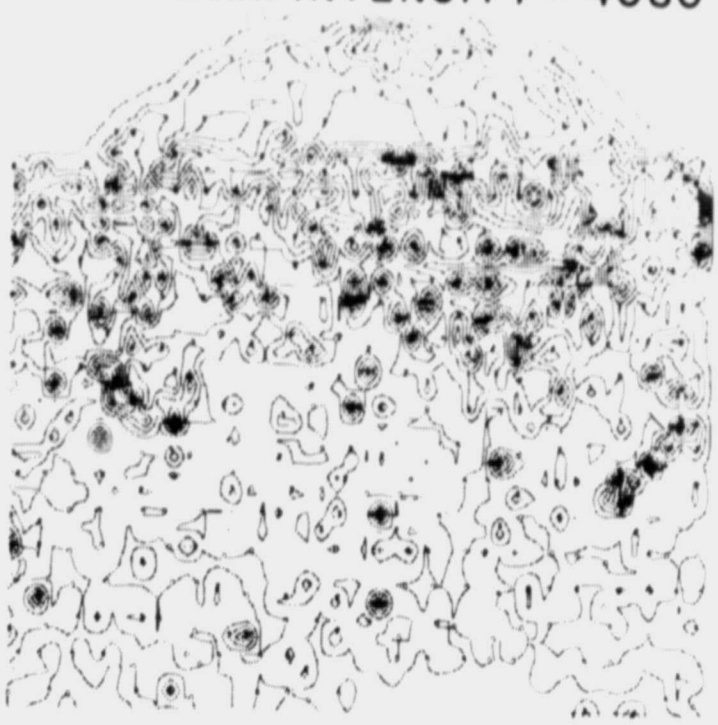

RASTER 4

RASTER 5

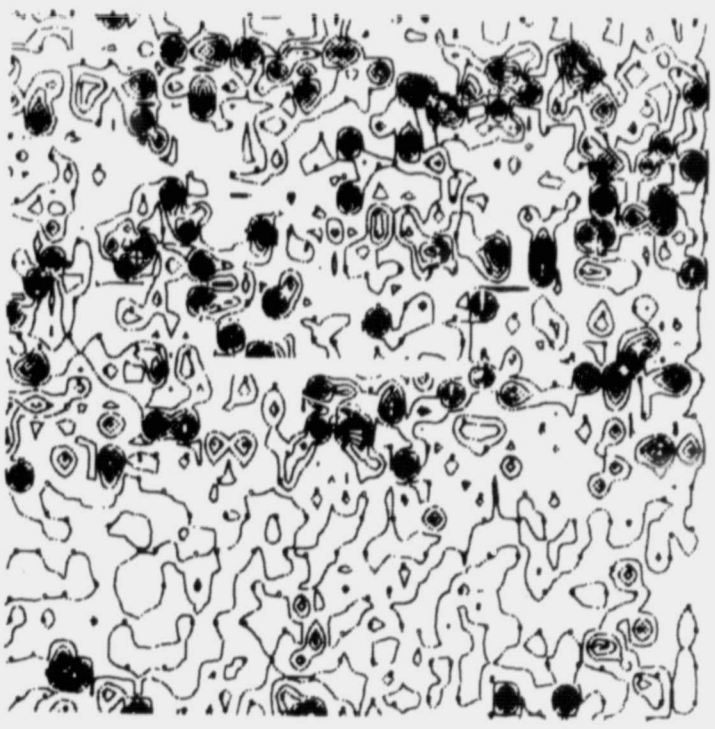

Figure 5B
RASTER PLOTS AFTER UV TERMINATION

indicate intensity by the dotted lines of constant intensity (isophotes). The highest data count recorded during each raster is printed above the raster picture as a maximum intensity figure. Raster 2 and raster 3 show the coherent solar images and very close correlation with expected intensities. Raster 4 begins at the top with a good rounded solar image, then the picture suddenly deteriorates as an image of the sun in ultraviolet light. The plots of raster 5 show no apparent relationship to a solar image.

The malfunction began in raster 4, line 9, word 13, at Universal Time 22 hr. 35 min. 11.5 (± 0.1) sec. on November 29, 1967. This is the mid-time of the readin gate (i.e. data acquisition period) whose data count was represented by word 13. The timing was established from the time signals contained in the final Harvard data tapes furnished by NASA. The satellite was passing over the Philippine Islands when the malfunction began.

The HCO main frame data words from the All-Channel computer printout for words 10 through 16 of line 9 are given in Figure 6 for rasters 2, 3, 4, and 5. These data were excerpted from the All-Channel playback received at the Johannesburg STADAN station toward the end of orbit 637.

WORD NO. IN LINE 9

RASTER NO.							
	10	11	12	13	14	15	16
2	00496C	00312C	00396C	00402C	00422C	00328C	00308C
3	00524C	00385C	00388C	00330C	00466C	00305C	00300C
4	00564C	00390C	00380C	*01248A	00976A	00786C	00632A
5	00024C	00028C	00038C	00004C	00108A	00108A	00014A

FIGURE 6

DATA WORDS BEFORE AND AFTER

UV TERMINATION

The numbers occurring in the data printout were programmed to be directly proportional to the number of ultraviolet photons incident on the photomultiplier of the HCO instrument from a selected portion of the sun at a specified wavelength. During all the raster scans taken during orbit 637, the instrument's spectrometer was set for 770Å. By reading down each column of Figure 6 one can compare counts recorded while the instrument pointed at approximately the same spot on the sun in successive rasters. Thus, for normal data there should be close correlation of the counts in each column. This is the case for the words from raster 2 and 3, and for raster 4 until word 13 in line 9. In that word the onset of the malfunction is signaled by the anomalously high count and by the appearance of an "A" following the count number rather than the usual "C". An "A" following the count number

indicates that the counter is registering less than 1.4 volts from the micro-switch circuit. The counts in words 14-16 of line 9 raster 4 are each more than twice as high as corresponding words in the previous rasters. During raster 5 the counts are very much lower than in previous rasters.

The count numbers from raster 4 and the four rasters following it were compared with corresponding counts from rasters 2 and 3 to determine whether or not the HCO instrument was transmitting any significant ultraviolet data underlying the noise, after the malfunction point. This would help to determine the condition of the high voltage power supply and detector. The comparison was made by using a computer to plot the average count for each data main frame (which contains four Harvard data words) on a logarithmic scale vs. time for the several rasters in orbit 637. Then the plots for rasters 2 and 3 were overlayed on the plots of corresponding points of subsequent rasters. These plots are shown in Figure 7.

The zero in the time scale in Figure 7 refers to the end of read-in time for word 3 in line 1 of raster 4. This coincides with the beginning of a data main frame. Since a raster takes 307.2 seconds to complete, the first time indication in Plot B refers to word 3 in line 1 of raster 5. Plot A shows the comparison between average data counts from lines 1 through 11 of raster 4 with averages from the corresponding lines of raster 2. These data are closely correlated until the malfunction occurs. Plot B shows a similar comparison of the initial lines

of raster 5 with those of raster 3. A review of these and other data have led to the conclusion that there is no significant correlation between the data counts recorded after the malfunction point and corresponding data obtained before the malfunction occurred. Therefore, all counts after word 13, line 9, raster 4 of orbit 637 are considered to be noise with the possible exception of the first six seconds after word 13. (Also see the computer raster plots in Figures 5A and 5B.)

As previously mentioned, another characteristic of the instrument malfunction is the presence of "A's" following the count numbers. Appendix I describes the conditions under which an "A" would normally appear in the All-Channel data; i) when the grating is in the Mechanical Reference position; ii) during the first four words at the beginning of a raster scan; iii) during the satellite night; iv) when the low voltage power supply of the instrument is off. Since none of these conditions existed at the time of malfunction, the spurious A's in the data are designated as false Mechanical Reference (MR) indications.

About 14 seconds after the onset of the malfunction, the Sail Analog Subcommutator read out the HCO high voltage current. The reading indicated 15.8 milliamperes (ma), close to the maximum 16 ma value allowed by the current limiting circuit design of the high voltage power supply for an overloaded condition. Normally the high voltage (HV) current readings ranged between 8 ma to 11 ma depending on temperature. After the malfunction

the HV current readings remained in an abnormally high range.

Readings of the HV current monitor and the five other HCO Analog Channels recorded during orbit 636-637 are plotted in Figure 8. The zero time indication again refers to word 3 in line one of raster 4. The readings plotted above each time mark were recorded during the 30.72 seconds following the time indicated. The scales on the left side of the plot refer to the digital values contained in the All-Channel data printout. The scales on the right were derived from calibration curves for the HCO Analog Channels.

The scale on the right of the ΔT plot should be regarded as an approximate indication rather than as an accurate scale because of calibration errors. The ΔT reading varies cyclically during each orbit because the satellite spends about one-third of each orbit in the earth's shadow.

The grating position parameter of Channel No. 4 does not indicate the grating position at night because the analog voltage read across the potentiometer is reduced by loss of both the +19V day power from the satellite and the -3V of the instrument's low voltage power supply. The low voltage power supply is off during the night portion of the orbit. The value of the Channel No. 5 readin gate parameter is higher at night than during day operation because the readin gate continues while the -5.5V from the low voltage supply ceases. The Channel No. 6 parameter pulse amplifier output has a low night

value because it loses the +4.2V of the low voltage supply at night.

The only analog parameters which deviate significantly from normal values at and following the UV data termination are the pulse count and the HV current readings. The pulse count readings after UV termination are difficult to interpret but can probably be attributed to low noise counts during the time when the parameter averaged (160 μs.). The HV readings will be discussed in Section 5.

4.2 POST-TERMINATION MODES

The HCO high voltage current monitor is read out once every 48 data main frames (MF), i.e., once every 30.72 seconds. (One of the 48 Sail Analog Channels is read out during each data MF. 30.72 seconds = 48 MF x 0.64 sec/MF.) For this analysis it is convenient to adopt 30.72 seconds as the basic interval of time for comparison of the HV readings with the other important parameters such as: average noise counts per word, number of zero counts, and number of false MR indications. These parameters are plotted in Figure 9. As in Figures 7 and 8 the zero on the Time axis refers to word 3 in line 1 of raster 4. The values plotted above each time mark are calculated for the 30.72 sec. following that time. After UV data termination two basic modes of operation can be distinguished. In Mode I noise counts in the main data words and false MR indications occur, zero counts are scattered, and the HV

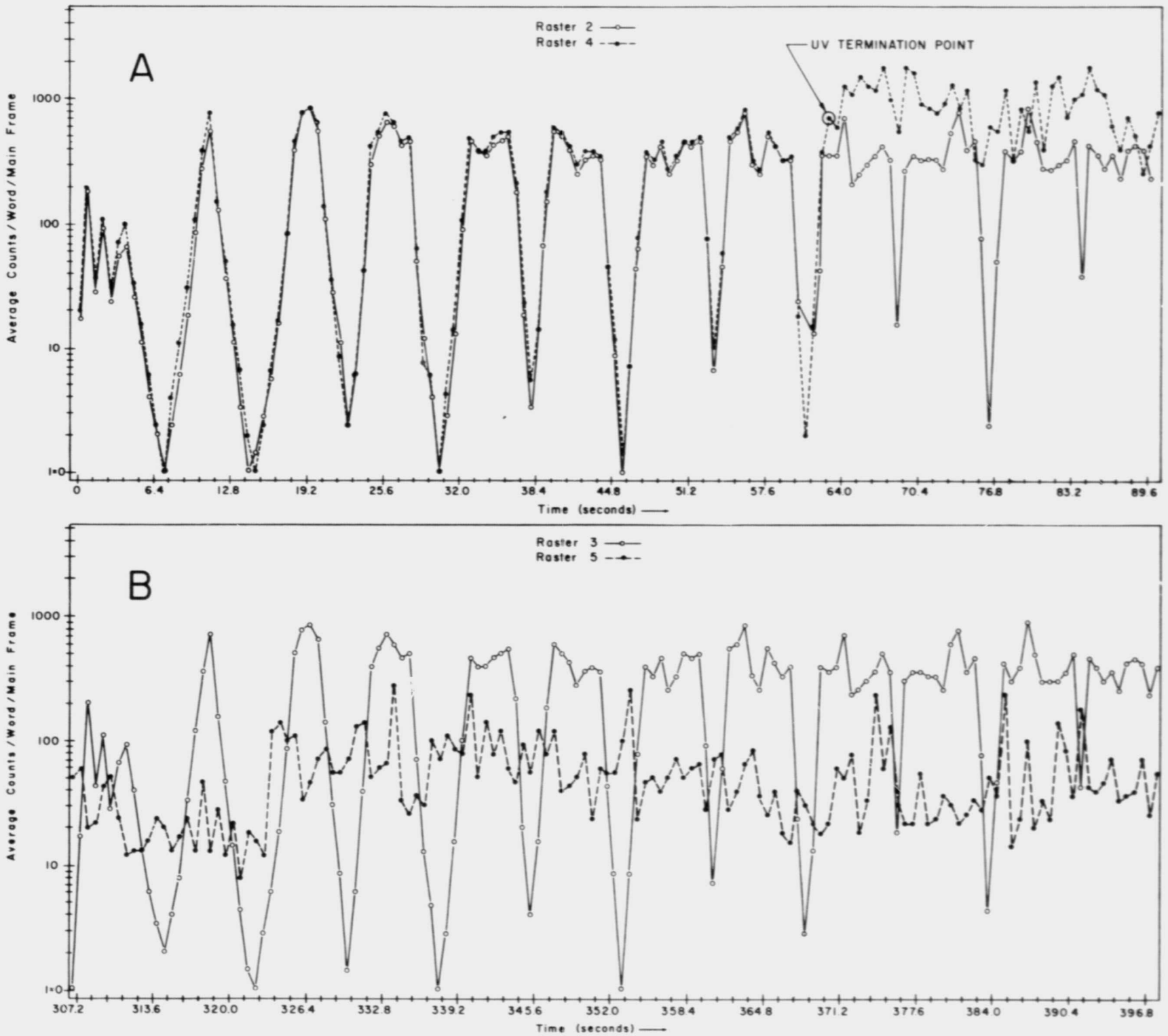

Figure 7 — DATA COUNT COMPARISONS
NEAR TIME OF UV TERMINATION

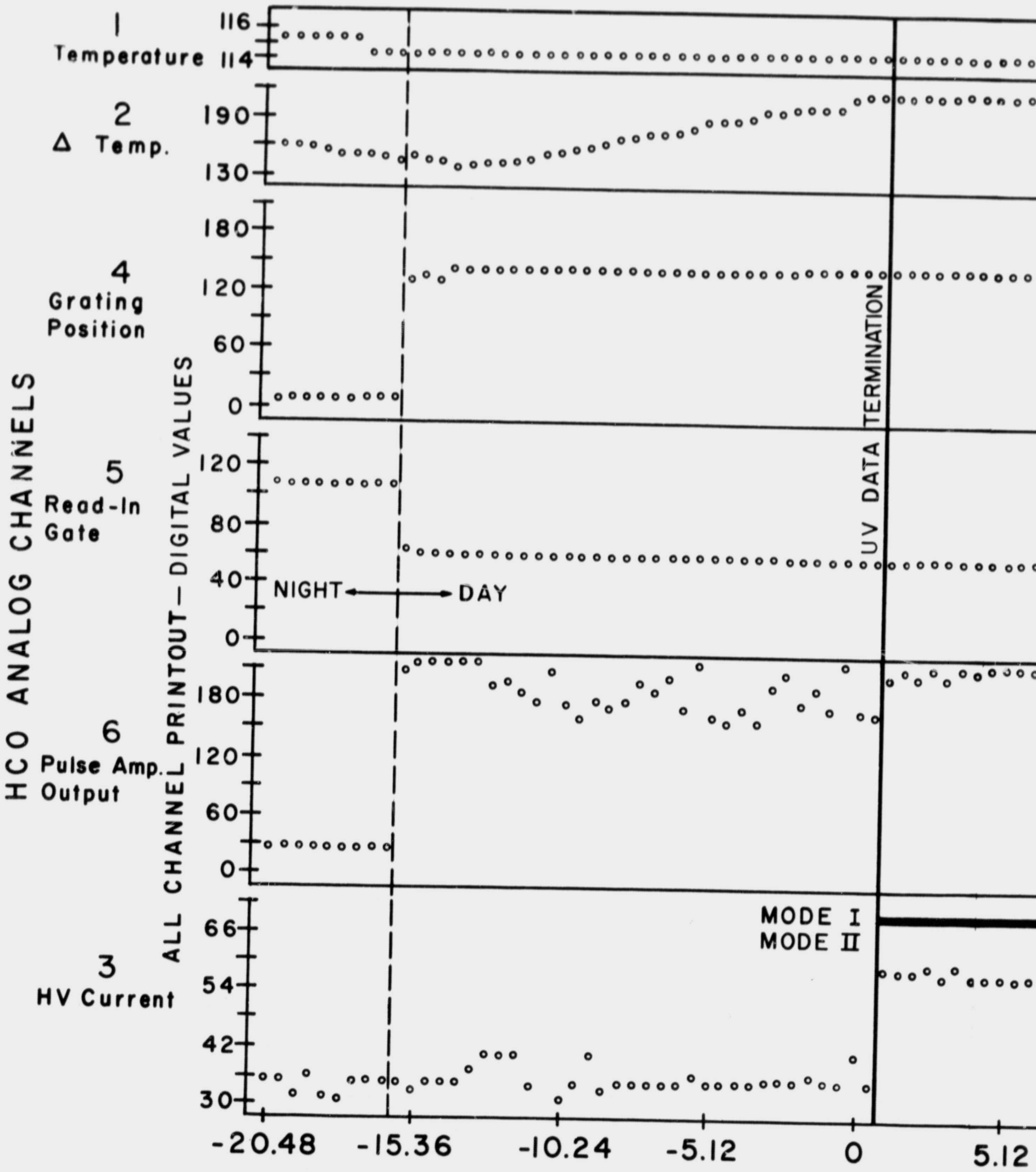

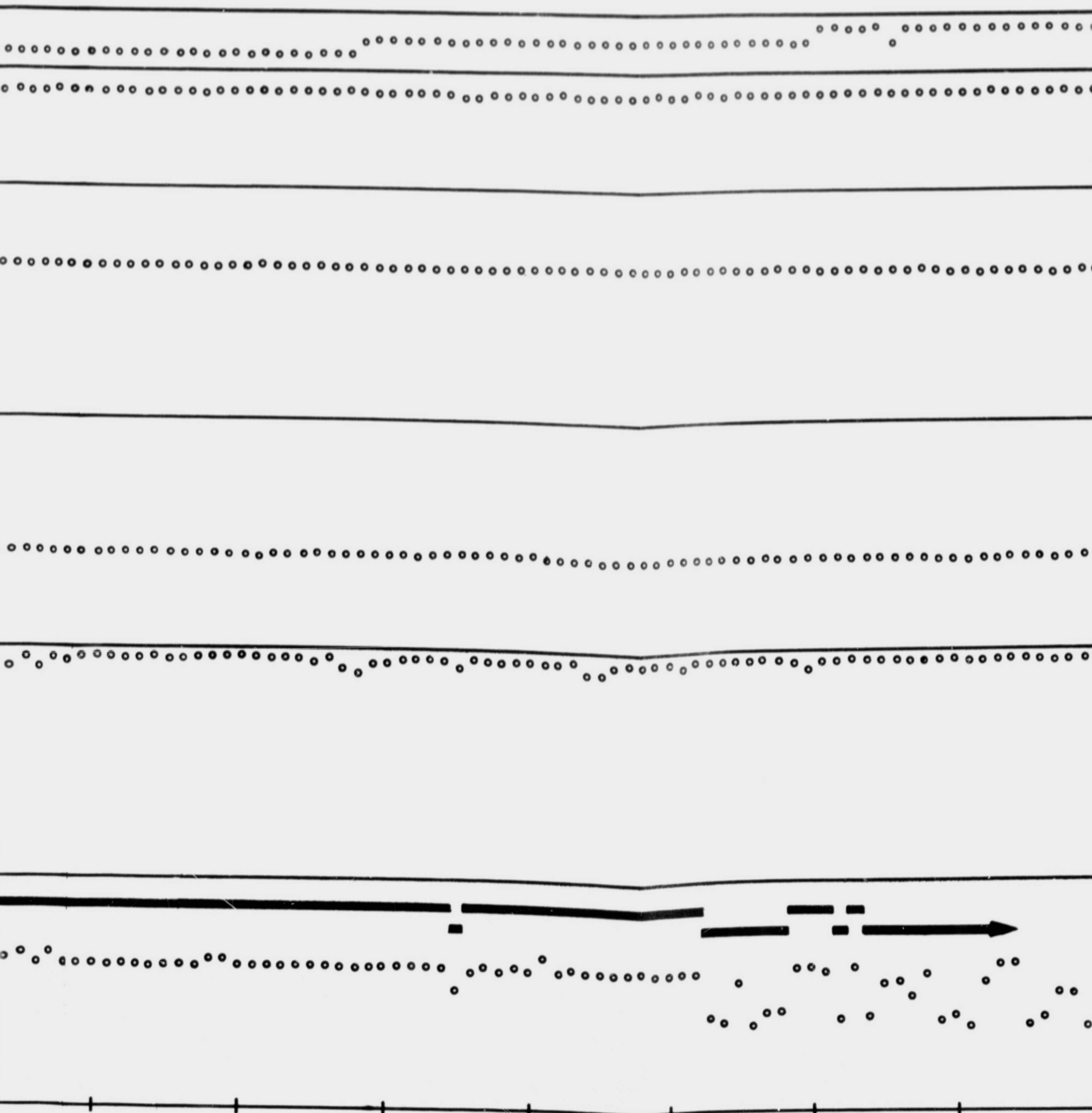

Figure 8 – HARVARD ANALOG DATA ORBIT 6

2 FOLDOUT FRAME

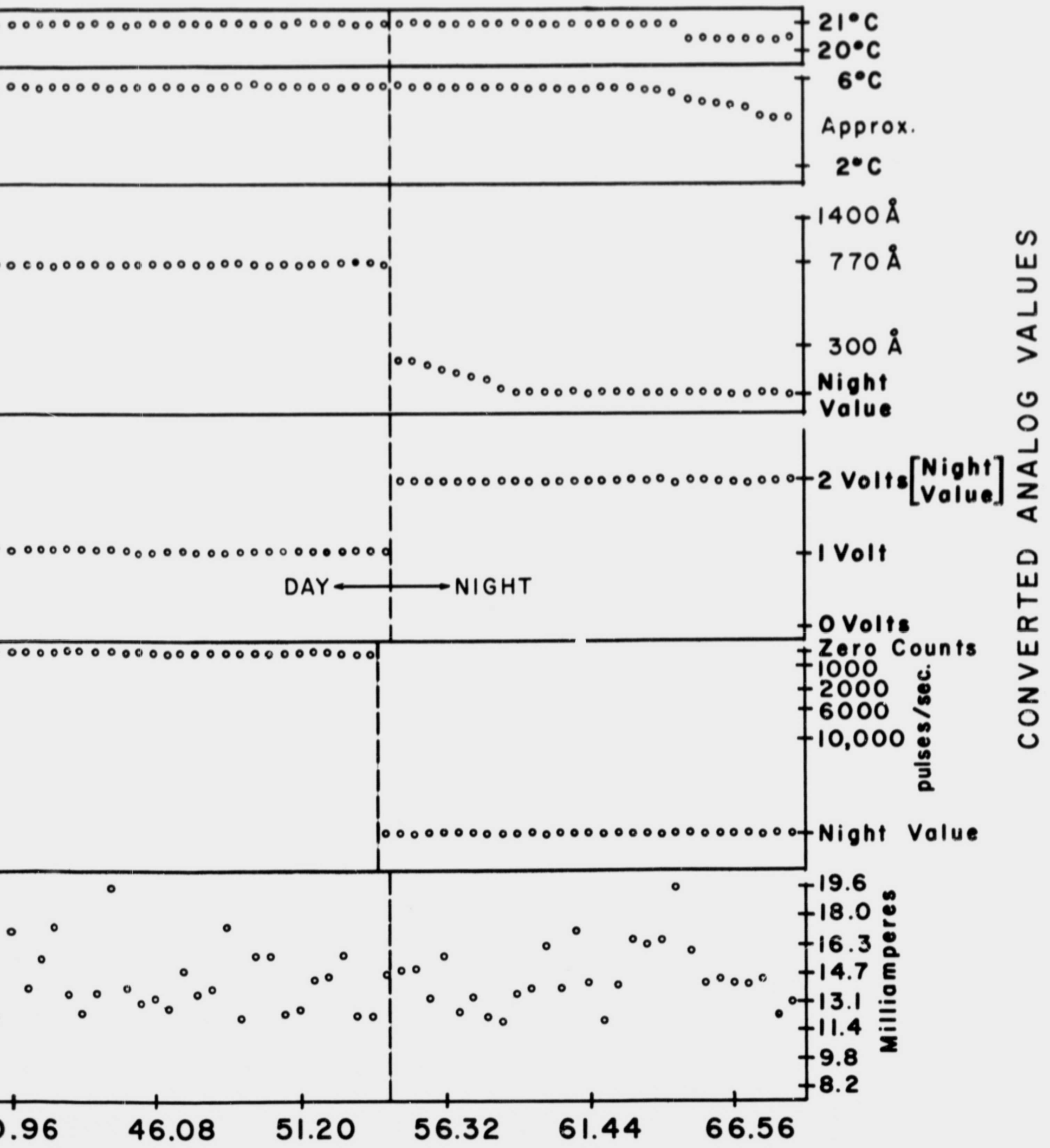

636-637

Figure 9 – HARVAR

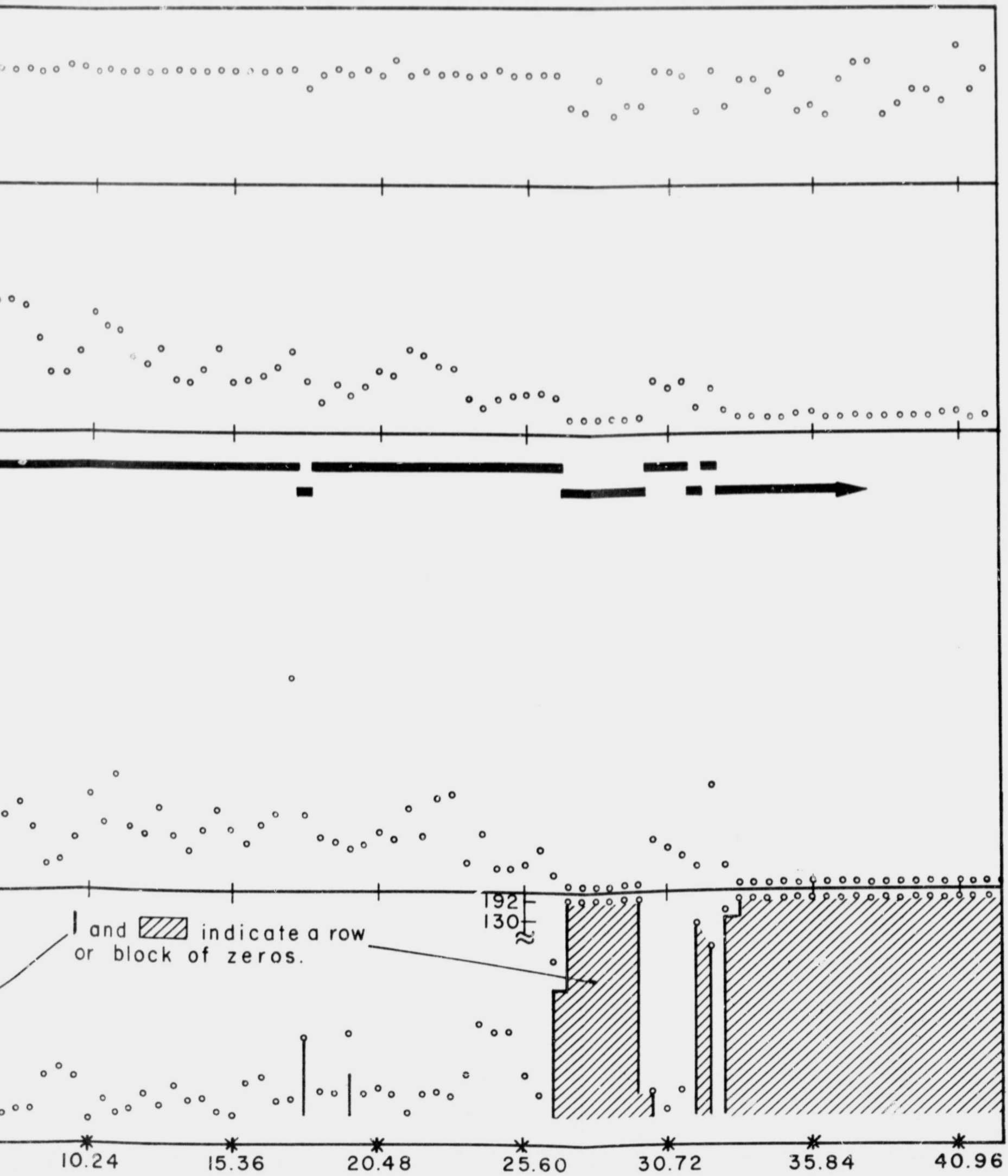

– HARVARD DATA – ORBIT 637

current reading remains fairly constant near the maximum value of 16 milliamperes allowed by the power supply circuit. In Mode II data counts in the main data words are consistently zero and false MR indications do not occur. HV readings remain higher than normal but fluctuate widely.

At the point of UV data termination the instrument changed from normal operation to Mode I operation. Within one minute a series of nine "00000C" printout data words followed by noise counts and false MR indications indicated a possible transition to Mode II and back to Mode I. Unfortunately the HV monitor was not read out during the occurrence of the zeros. About 17 minutes after UV termination a series of thirty-two "00000C" data words occurred. The HV monitor was read out during the series of zero counts. The HV monitor reading was significantly lower than Mode I readings. Here we have a clear indication of a transition to Mode II for about five seconds then back to Mode I. A minute later a series of eighteen "00000C" words indicate another possible occurrence of Mode II (see Figure 9) followed by Mode I. About 26 minutes after UV termination the instrument went into Mode II operation for 3 minutes. This was followed by 1 minute of Mode I, 30 seconds of Mode II, 30 seconds of Mode I, and finally, Mode II. The instrument continued in Mode II until it was turned off fifteen hours later during orbit 646.

4.3 LATER SIGNIFICANT ORBITS

It was mentioned earlier that during the three months following the failure (through late February 1968)

the high voltage system was occasionally turned on, first very cautiously and then systematically, in the hope of initiating some change of state in the system. On only three occasions was there evidence of a brief change in mode. The first two occurred within one day of the malfunction, and the third was on January 8, 1968.

During orbit 649 the HV power supply was turned on for one minute. Count noise and false MR indications which occurred throughout the period indicate Mode I operation, but the two HV monitor readings taken during that time are not characteristic of Mode I. Data recorded during the "HV on" period are plotted in Figure 10.

In orbit 650 the HV power supply was turned on for 3 minutes 30 seconds. Count noise and false MR indications appeared during the first six seconds. After that zero counts, the absence of false MR indications and high, fluctuating HV monitor readings indicate Mode II operation until the instrument was turned off. These data are plotted in Figure 10.

Five weeks later on January 8, 1968 during orbit 1238 the HV power supply was turned on for 2 hours and 50 minutes. For 1 minute and 45 seconds noise counts, false MR indications, and high, constant HV current readings indicate Mode I operation. This was followed by one minute of Mode II, three minutes of Mode I, then Mode II until the HV was turned off. Figure 11 shows plots of data from orbit 1238.

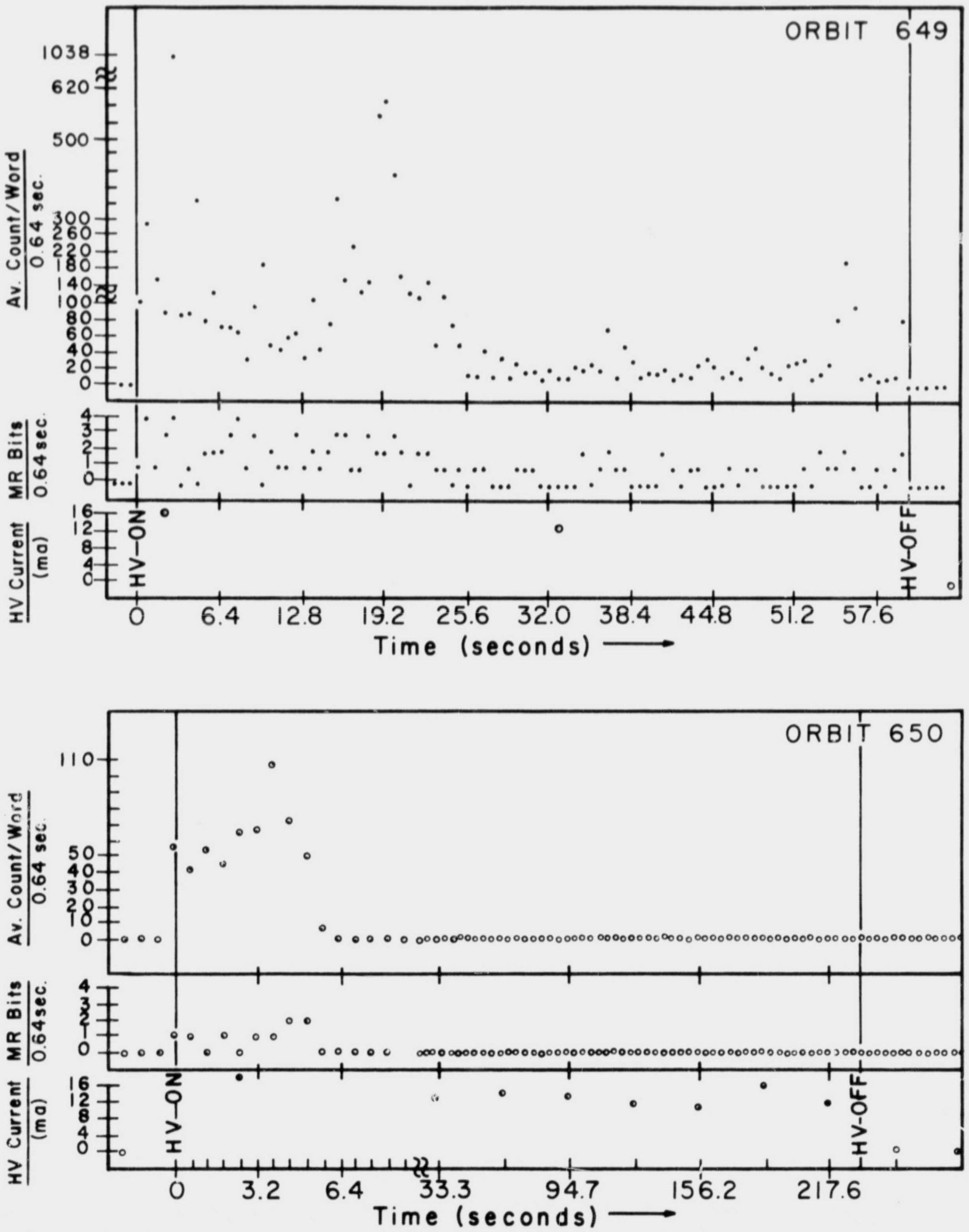

Figure 10—HARVARD DATA—ORBITS 649, 650

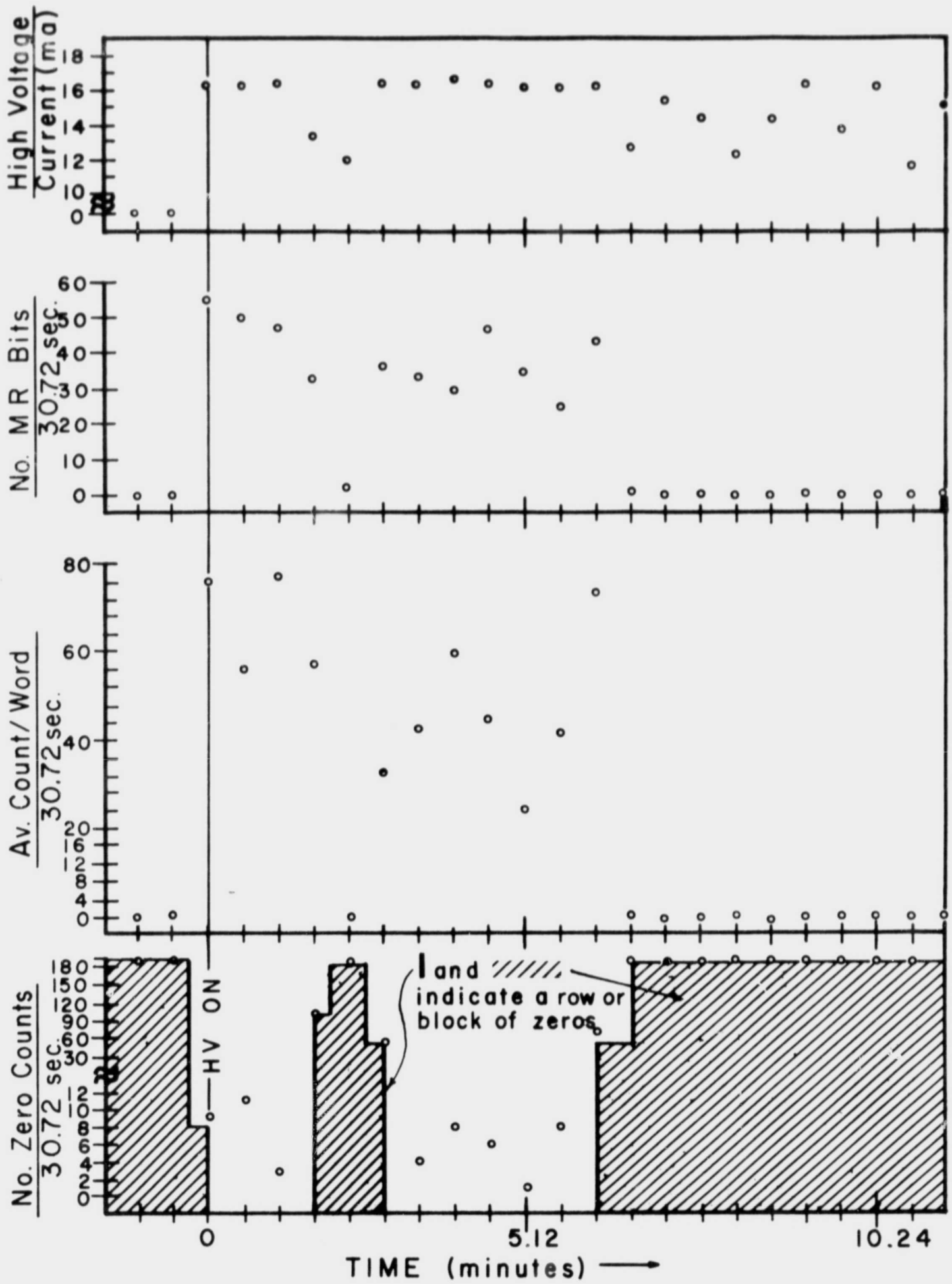

Figure II—HARVARD DATA— ORBIT 1238

5.0 ANALYSIS

5.1 DATA STUDIES

Now after we have described the data, we will attempt to interpret them. One begins by noting that the All-Channel printout data of other experiments in OSO-IV show no drastic change at or shortly after the UV termination of the HCO instrument. We therefore conclude that the spacecraft's telemetry system did not cause the difficulty, and further that it did not originate in another experiment. The noise counts and false MR indications which appear in the printout must originate within the HCO instrument itself: more specifically in the counter, pulse amplifier, pre-amplifier, photomultiplier, voltage divider, or high voltage supply (see Figure 3).

A block diagram of the counter in the HCO instrument is presented in Figure 12. The signal from the pulse amplifier arrives at the count input in the upper left corner of the diagram. During the 80-millisecond (ms) readin gate signal the inhibit generator is prevented from operating, and the input gate circuit is made operable, allowing the counter stages A', A, B, and C to count incoming pulses. Following the end of the readin gate signal the counter remains inactive for 40 ms. Then the readout gate signal from the spacecraft activates the shift generator for 40 ms. During that time the "1's"

and "O's" stored in the A, B, and C counter stage, the mechanical reference flip-flop, and the optical reference lines are shifted out serially to the spacecraft's telemetry system. Then the cycle begins again with a readin gate signal.

How did the noise counts and false MR bits that appear in the data printout get into the counter? The noise counts immediately after the malfunctions are high compared with expected count levels. They are low compared with the capacity of the counter ($2^{15}-2 = 32,766$). If the noise were present in the inhibit generator or shift generator, it seems reasonable that the noise would excite a "1" state in any of the counter stages with equal probability. Since the highest count recorded after UV termination was 4,080, and since the average count per word remained comparatively low and generally decreased after UV termination (see Figure 9), we infer that the noise did not come from the inhibit generator or the shift generator. In that case, the noise must have arrived at the counter from the count input.

A similar argument can be made concerning reference bits. Only "A" and "C" corresponding to reference bit binary "11" and "10" respectively (see Appendix 1) appear as reference indication in the post-termination printout. "B" and "D" (binary "01" and "11" respectively) do not appear. Therefore after UV termination the optical reference

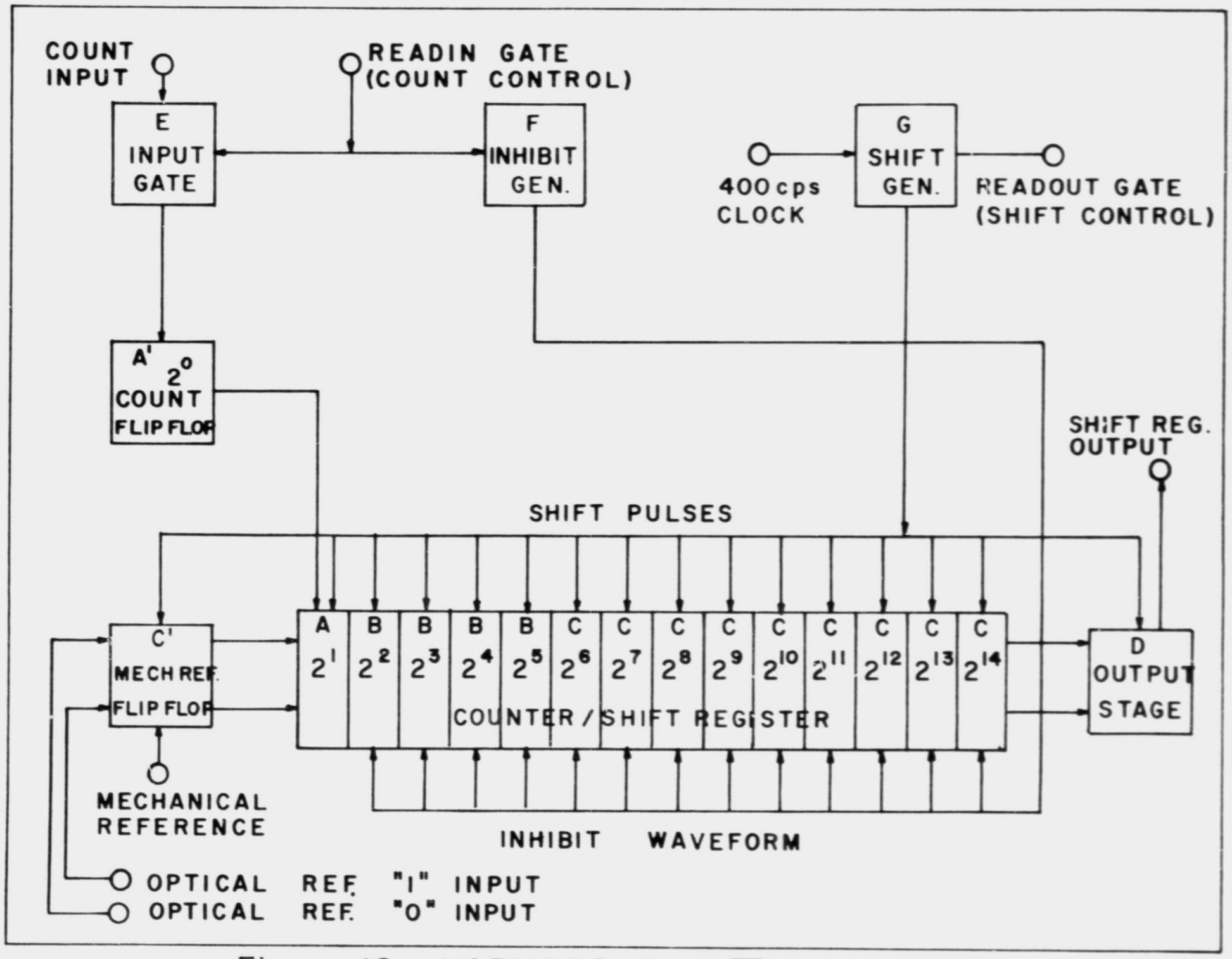

Figure 12 – HARVARD OSO-Ⅳ COUNTER
BLOCK DIAGRAM

bit remained in the "O" state that it had maintained during the rasters before termination. From this constancy we infer that the noise which produced spurious "A'S" in the printout did not enter the mechanical reference flip-flop through the optical reference lines. Since we have already eliminated the shift pulse line as a source of noise, the reference bit noise must have entered the MR flip-flop through the mechanical reference input line. Thus, the noise in the instrument was recorded in the counter but did not originate in the counter.

5.2 LABORATORY STUDIES

Soon after the malfunction an effort was made to simulate in-orbit conditions in the laboratory. This was done on the prototype instrument, which was made to be a good representation of the flight unit. The excessive high voltage primary current, evidence of noise in several places in the instrument, and loss of detection performance all suggested the possibility of high voltage breakdown within the instrument. Therefore, the studies were concentrated on simulating the observed orbital data by artificially introducing breakdown paths in a variety of places and by subsequently creating simulated component malfunction.

Appendix E of Experimenters' Manual for the OSO, Supplement #IV (see Appendix II of this report) contains

a brief description of the physical mechanism responsible for breakdown phenomena:

> The 'breakdown' of a gap between electrodes surrounded by a gas occurs when free electrons in the gas (a few are always present due to ionization by background radiation) are accelerated by the potential gradient to a high enough velocity to ionize atoms or molecules with which they collide. For a given pair of electrodes, the spark-over voltage decreases almost linearly with pressure until the mean free path of the electrons becomes comparable with the electrode spacing, where the spark-over voltages reach a minimum and increase again with further reduction of pressure.
>
> The minimum voltage depends on the type of gas present and the nature of the electrode surfaces and usually is in the range of 200 to 400 volts. This occurs at a pressure in the neighborhood of 1 millimeter of mercury. The potential gradient will be high in the neighborhood of sharp points on conductors or small diameter wires, and ionization or corona near the conductor surface can occur without an actual spark-over. Ionized gases are frequently chemically active, and often tend to react with and degrade organic insulating materials, causing permanent leakage paths. In this case, breakdown may occur only after a considerable length of time under stress.
>
> In radio-frequency circuits, a second breakdown region may occur at much lower pressures (order of 10^{-2} to 10^{-3} mm Hg), and somewhat lower voltages. The mechanism of ionization here is different, and involves mainly emission of electrons from the surface of the electrodes.

As a result of earlier experiences by HCO, a considerable amount of effort during the development of this instrument was devoted to eliminating damaging effects of spontaneous or self-induced corona. After the elimination of several design weaknesses, the final

configuration was qualified (with the prototype instrument) by being subjected to nearly continuous spontaneous corona in ambient pressures varying between 0.01 and 0.2 torr, for many hours. Although the testing was visually spectacular, subsequent operation showed that the instrument was not catastrophically damaged by the test. (No attempt was made to ascertain if any changes occurred in the photometric detector efficiency). Data taken during this corona testing showed that the current in the primary side of the high voltage power supply was the maximum (approximately 16 ma) allowed by the current limiting transistor (Q1 in Figure 13). Self heating of that transistor caused a slight decrease in the maximum current, and changes in corona mode induced slight current fluctuations. The high voltage current readings obtained during Mode I operation in the first 26 minutes after the instrument malfunctioned (see Figure 9) have exactly the same characteristics.

As in the pre-launch corona testing, the prototype instrument was not damaged by artificially induced short circuits at atmospheric pressure during the laboratory studies. To investigate further the possibility of component damage in the orbiting instrument, the count input line was disconnected from the counter in the prototype. When the instrument was subjected to short circuits in the laboratory, no counts were recorded in the counter. Then, with the count

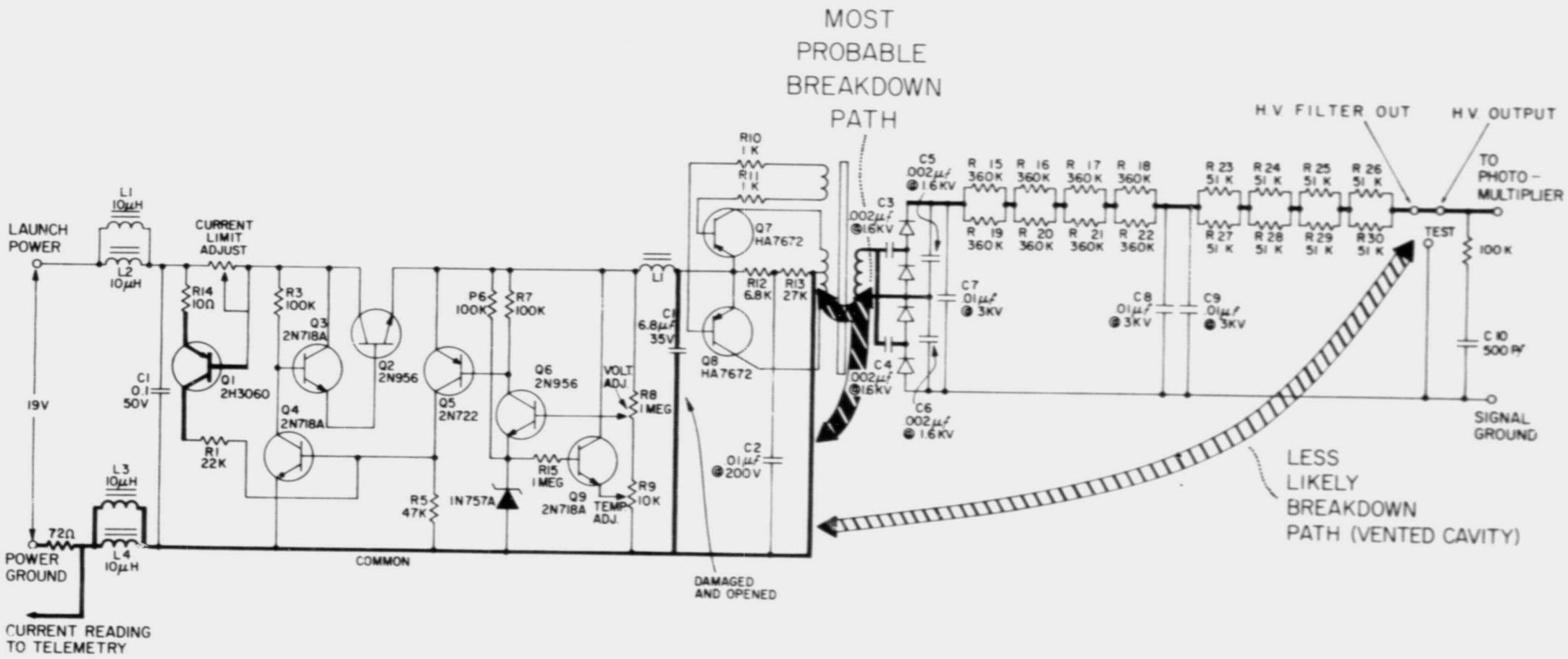

FIGURE 13 – HIGH VOLTAGE SUPPLY

input line reconnected, the power line to the pulse amplifier was disconnected. Again when the instrument was subjected to short circuits no counts were recorded. However, with power returned to the pulse amplifier and the input from the preamplifier disconnected, counts were recorded when short circuits were induced within the instrument. Thus it was concluded that the pulse amplifier was operating after the UV termination.

5.3 MODE I

With the major components properly connected, high voltage breakdown was induced from the HV terminals to points in the photomultiplier, in the interface between the preamplifier and the pulse amplifier, in the high voltage cable and connector to the voltage divider, and in the high voltage supply itself. High voltage breakdown at all points tested produced random noise counts in the counter and maximum current in the primary side of the HV supply. However, only HV breakdown within the HV supply between a high voltage lead and the common line on the primary side (see Figure 13) produced false MR indications in addition to the maximum current and count noise. These three characteristics appearing together are indicative of Mode I. These tests seem to rule out the photomultiplier voltage divider, HV filters, and other items as being involved in the malfunction.

In Section 5.1 we described that false MR indications were produced by noise on the mechanical reference input

line to the MR flip-flop in the counter. To see how noise on the MR line could be produced by HV breakdown to the common line in the HV supply we follow the common line back to the Matrix Box where the 72Ω resistance connects the common to power ground. The Sail Analog Subcommutator samples the voltage across that resistor once every 30.72 seconds to monitor the current flowing in the HV power supply. Within the Matrix Box the HV common line and the mechanical reference line are in close proximity. Studies on the prototype instrument indicate that a voltage of 1.4 or greater applied to the MR input line would trigger the "O" condition in the MR flip-flop, and thus produce an "A" in the All-Channel printout. HV breakdown in the laboratory between a high voltage lead and the common line produced pulses of 200 volts (with respect to power ground) on the common line, and tests indicate that pulses of this amplitude of a few microseconds duration on the common line are sufficient to trigger the MR flip-flop. Thus, breakdown between a high voltage source and the common within the power supply appears to have induced (within the Matrix Box) the noise that appeared on the MR input line during Mode I operation.

Review of the geometry within the HV supply has shown that the high voltage is physically close to the common at two locations: i) within the high voltage transformer between the primary and secondary windings, and ii) in a vented cavity between a printed circuit mother board and

the high voltage connector terminal. These places are shown as possible breakdown paths in the HV supply schematic in Figure 13. Section 5.4 will provide more detail on the transformer and the printed circuit board. We can tentatively explain Mode I operation as the result of HV breakdown along one of the paths illustrated in Figure 13.

5.4 MODE II

Mode II operation with its zero counts, absence of false MR bits, and high, fluctuating current was more difficult to simulate than Mode I when a high voltage lead was shorted to the common line, the noise counts and false MR bits ceased, but the current level remained at the maximum allowable level without fluctuating enough to produce the readings observed in Mode II. Only when the low voltage capacitor (C1 in Figure 13) was opened while the high voltage was shorted to common did substantial current fluctuations appear.

Capacitor C1 is a 6.8 microfarad tantalum unit with a 35-volt rating. Although its rating is compatible with the basic circuit requirement, laboratory tests have shown that these capacitors became open circuited when a 90-volt potential of the proper polarity was applied. But capacitors of this type are also very susceptible to reversed polarity exposure and fail at a very few volts potential.

Transients on the common can very well have been of both forward and inverted polarities with respect to the capacitor. Given the magnitude of the observed

pulses on the common during laboratory test in the prototype, we consider it likely that similar pulses produced by corona breakdown in the orbiting instrument opened the C1 capacitor.

Possible involvement of the transistor Q4 (Figure 13) was not studied in the laboratory. There is reason to believe that it would have the same degree of susceptibility to transients on the common line, although it might be more apt to recover after such an event. The loss of this transistor would produce loss of regulation and oscillation of the supply. Although the detailed telemetry record might be somewhat different, the rationale of the mode definitions and transitions would not change materially if such a failure were considered; hence we will continue to refer to capacitor C1 in subsequent material.

Laboratory tests indicated that Mode I characteristics including count noise, false MR indications, and fairly steady maximum HV current readings result when breakdown is induced between a high voltage lead and the low voltage side of the common line. Further tests showed that Mode I characteristics continued to result from such breakdown even when the C1 capacitor was open. We conclude that C1 could have opened anytime during Mode I operation.

With capacitor C1 open, Mode II operation (zero counts, no false MR bits, and high, fluctuating HV current) results when a short or a leakage resistance of less than 4 megohms is introduced between the high voltage and the output common line.

When the leakage resistance is greater than 4 megohms the primary current does not fluctuate sufficiently to be characterized as Mode II operation.

The high voltage current readings from a total of 44 orbits (in January and February 1968) are plotted in Figure 14. During these orbits Mode II conditions prevailed in the instrument. Illustrated in the upper right corner of Figure 14 is a current waveform obtained in the prototype instrument with capacitor C1 open and a high voltage lead shorted to the common line.

As mentioned previously, the analog subcommutator data sample is a period of 160 μsec., taken every 30.72 sec. For the purpose of this discussion it can be considered a brief sample (small compared to the period of the signal) and taken at random intervals. Although by no means conclusive, the sample distribution shown in Figure 14 can certainly be interpreted as a statistical sample of the waveform shown. Note that no readings were obtained below 11 ma (i.e., approaching the normal current range).

Assuming that C1 opened during Mode I operation (perhaps during the first minute after UV termination) we can tentatively explain Mode II as the result of a low resistance connection developing between a high voltage source and the common line. The alternation between Mode I and Mode II conditions can best be explained to have resulted from the time variant character of such a connection (e.g., transition between a corona breakdown and a short circuit).

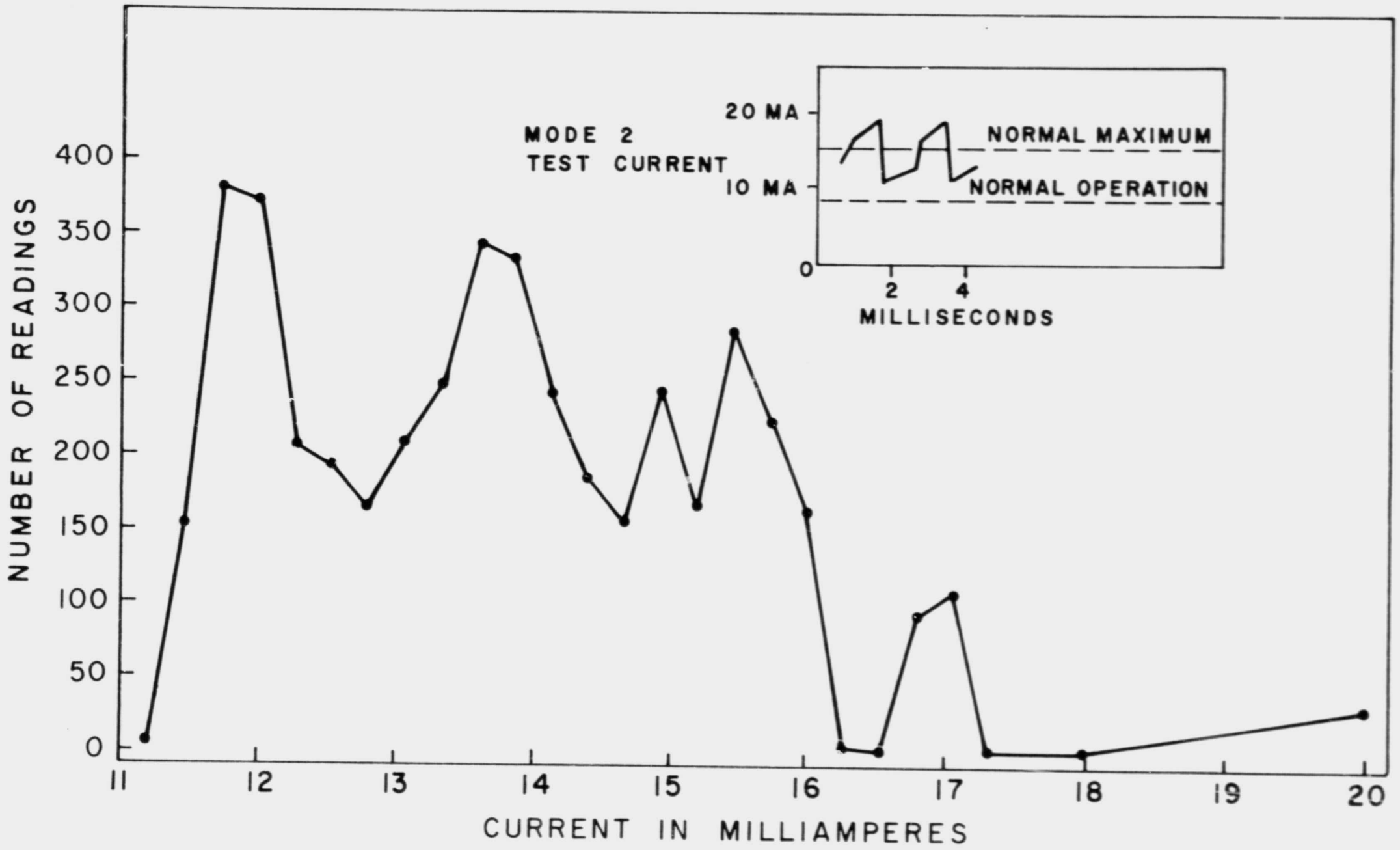

Figure 14— HV CURRENT READINGS (MODE 2)

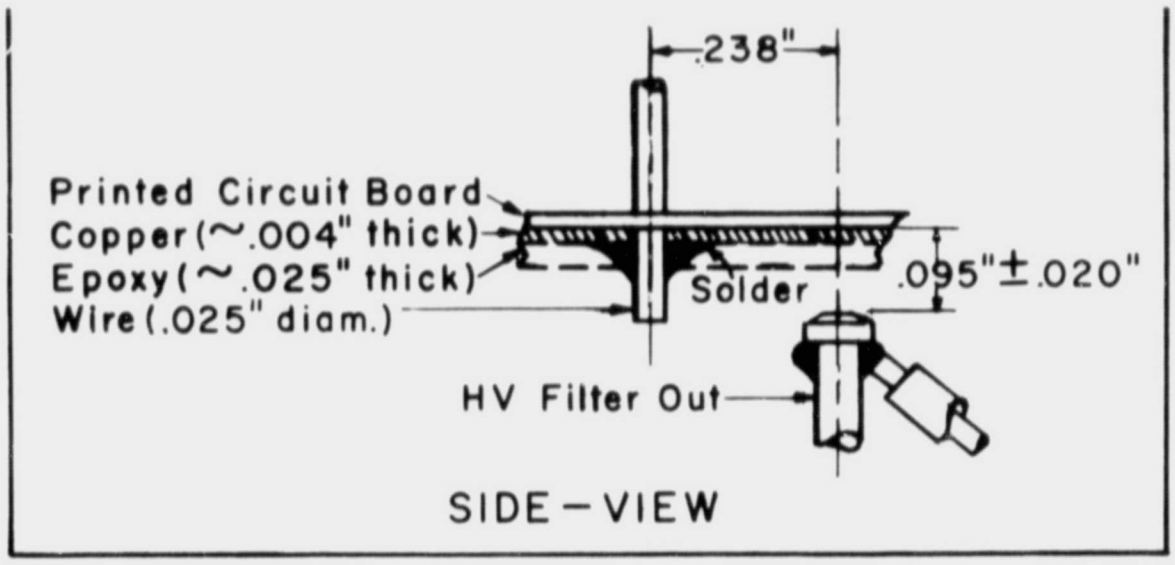

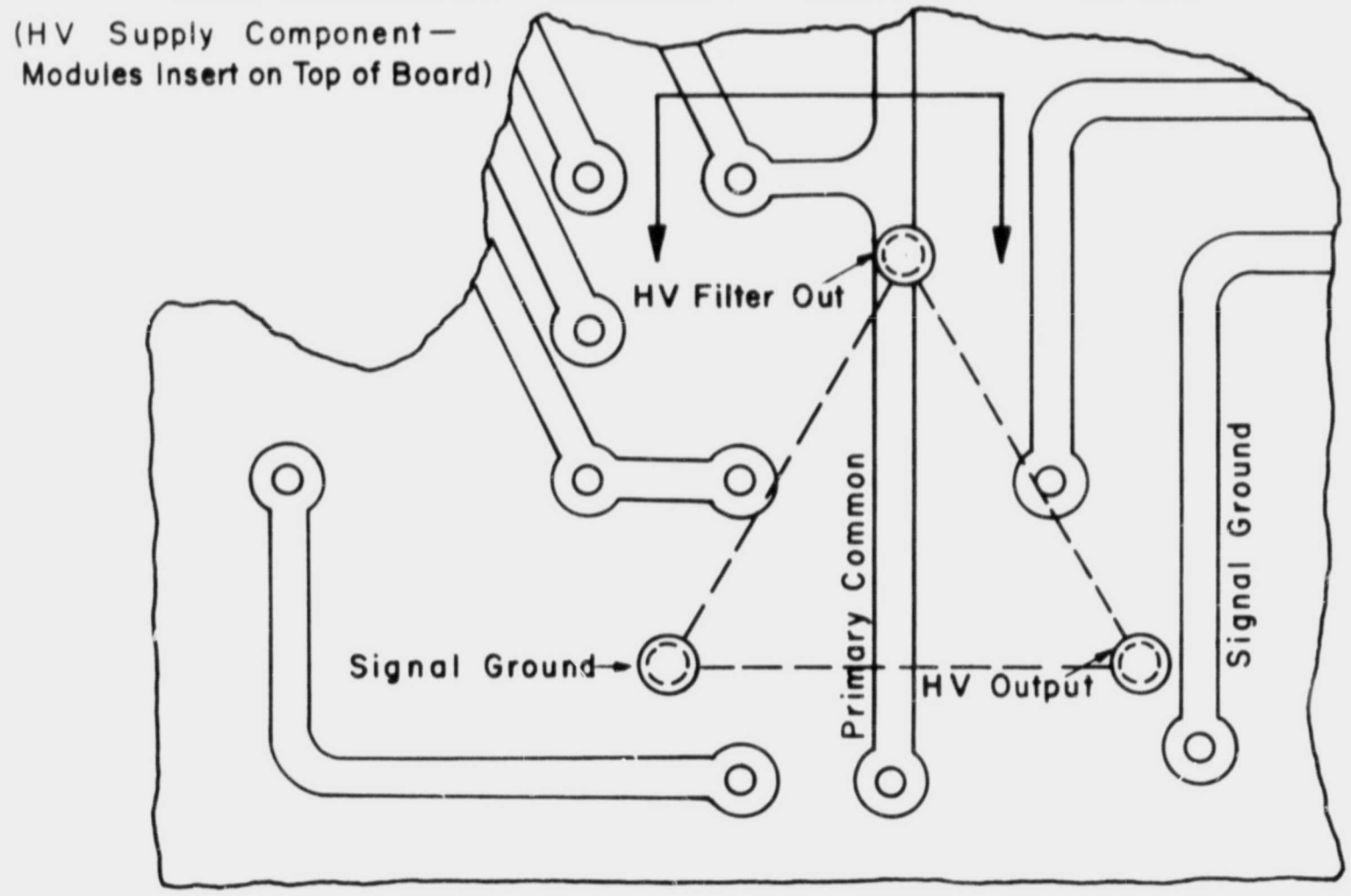

Figure 15 – HV PRINTED CIRCUIT

5.5 POSSIBLE BREAKDOWN PATHS

In conjunction with laboratory study and simulation of Mode I and Mode II conditions in the prototype instrument, an investigation of the physical arrangement of high voltage power supply components was made to determine possible breakdown paths. High voltage is physically close to the common line on the primary side in two locations: 1) at one pin of the flight-enabling connector near the output of the high voltage supply, and 2) within the high voltage transformer.

The photomultiplier is of open (windowless) construction. Since it is designed to operate in vacuum, high voltage applied to it under normal atmospheric conditions might cause a breakdown within it and possible damage to it. Thus, to check the high voltage supply before flight a special test connector replaced the photomultiplier load at the HV supply output. The test connector contains a 50 MΩ resistance load similar to the load of the photomultiplier. For flight the test connector was replaced by a flight-enabling connector containing a jumper lead between the two pins on the HV side of the output. The drawing in Figure 15 shows part of the main printed circuit board in the HV power supply. The dashed lines join the three connector pin junctions of the output network assembly. That assembly is attached to the inside of the bottom cover on the HV power supply box. The HV output pin is ~1/10" away from the copper signal ground line on the printed circuit board. Induced arcing between a HV lead and the signal ground line in the prototype instrument did not cause false MR indications to appear. So we infer that

arcing at that point did not cause Mode I operation.

The other high voltage point in the flight connector is pin labeled the HV Filter out. The drawing in the upper part of Figure 15 shows a side view of this HV pin and it demonstrates the proximity of a wire connected to the primary common and to a pin from the low voltage filter module. One could speculate that outgassing within the power supply box and deterioration of the conformal epoxy coating may have produced conditions sufficient to sustain a corona discharge between the HV Filter out and an adjacent low voltage point on the primary common. However, the HV supply was vented and was not turned on until six days after launch to insure proper outgassing of the HCO instrument (this seems to be a remote possibility). Also, with this explanation of Mode I operation we lack a mechanism for the low resistance or short suspected of causing Mode II operation.

We now consider the high voltage transformer. The toroidal core assembly used in this transformer is manufactured by GL Electronics (Part No. GL-A-4057-M1). The core tape is supermalloy foil and is embedded in a silicone grease within an aluminum housing. The housing is sealed by a crimp seal against a rubber washer backed up by a glass-laminate board. The housing is black anodized and has rounded corners. The silicone grease is used to protect the core from mechanical stresses on the box due to winding which might alter the magnetic properties of the tape. The grease also cushions the core during vibration and shock testing.

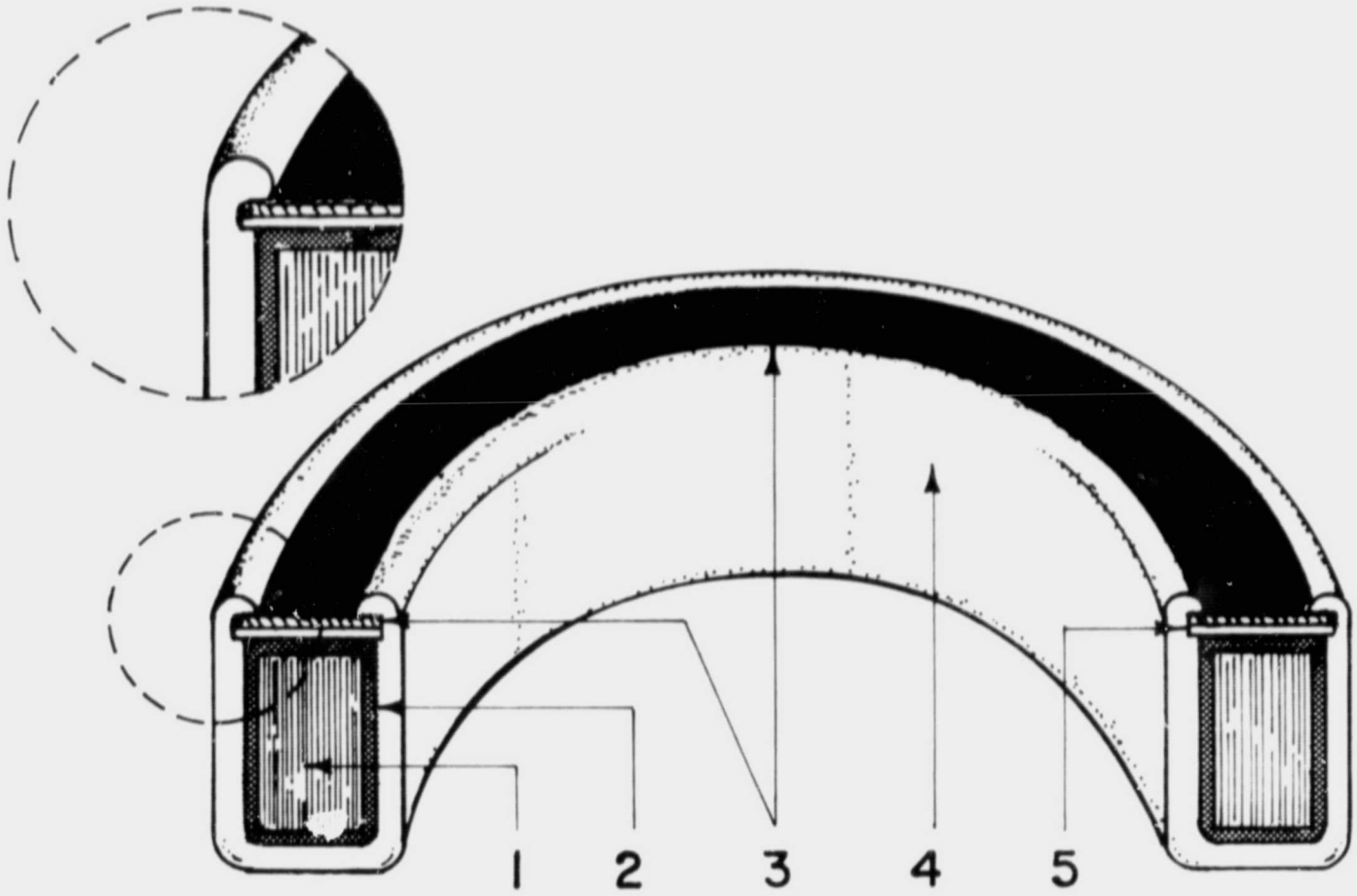

1. Core Tape 2. Silicone Grease 3. Rubber Gasket
4. Aluminum Case 5. Glass Epoxy Insert

Figure 16

HV TRANSFORMER CORE

The glass-laminate board serves to break the electrical path around the core box. The core construction is illustrated in the cut-away view of Figure 16.

A thin layer of TFE (Teflon) tape is wound around the core box for insulation. And the primary winding of enamelled copper wire is then applied uniformly around the circumference. The teflon insulated lead wires are attached and brought out radially. Another layer of TFE tape is wrapped over the primary winding although a gap is left in the area of the lead wires. The multi-layer secondary windings are then wound and leads are attached. TFE tape is then wrapped over the secondary windings.

The transformer assembly is conformally coated with RTV-11 silicone rubber which has been degassed in vacuum. It is then cured at room temperature, and baked at moderate temperature and atmospheric pressure. On the sample transformer examined in our laboratory a layer of RTV-11 between .010 and .030 inches thick was found which has not penetrated through the outermost layer of TFE tape.

The transformer is assembled into the transformer module and the entire module is then filled with C-7 encapsulant. The whole module is vacuum degassed at a pressure of ~20 torr and then cured at elevated temperature at atmospheric pressure.

Inspection of a sample module (see Figure 17) in our laboratory indicates that the C-7 did not penetrate through the RTV into the secondary winding area. However,

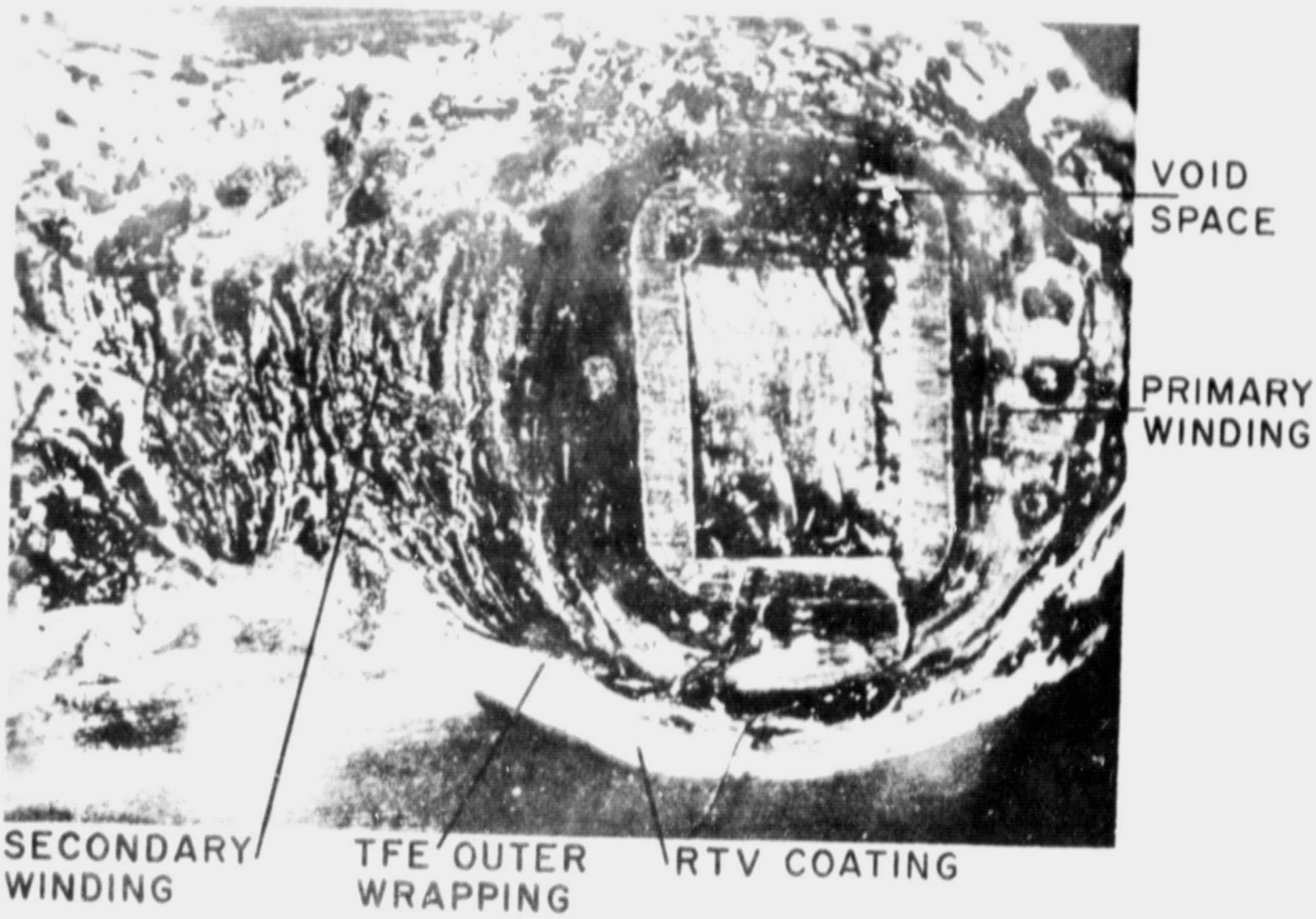

Figure 17 — UV TRANSFORMER CORE MODULE

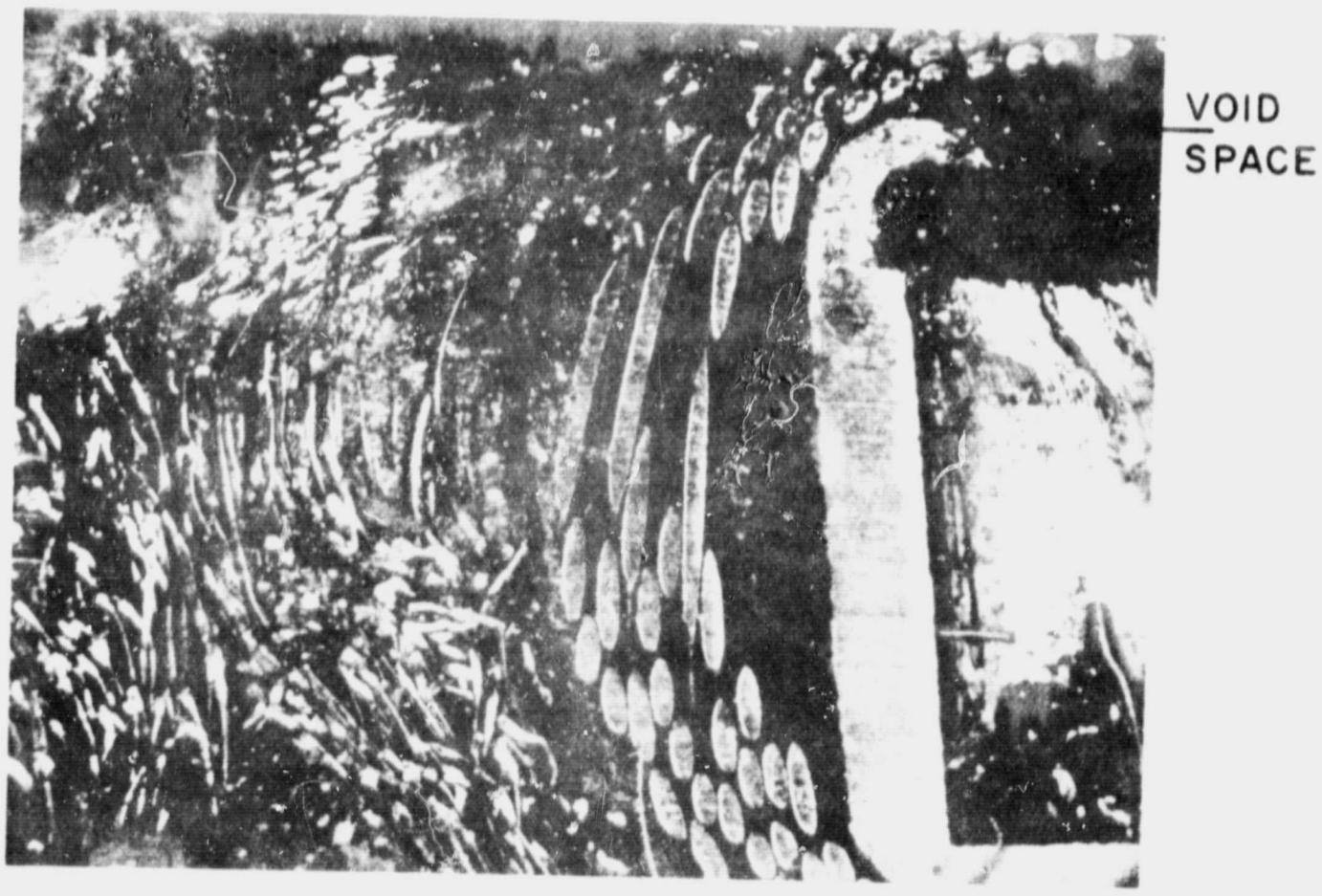

it did penetrate down the primary leads and partially encapsulated the primary winding. The manufacturer of the HV power supply said that this was a random occurrence. In our sample the C-7 had not bonded to the aluminum box of the core. The TFE tape winding on the core box was stretched across the top of the rolled aluminum edges on the core box and this created a void space between the rubber washer seal of the box and the TFE tape.

The encapsulation process included degassing the module at a pressure of approximately 20 torr. After degassing and restoration of atmospheric pressure the C-7 encapsulant presumably backfilled some of the spaces which under vacuum conditions were of the residual gas trapped inside the transformer. It appears that a significant volume of air at a pressure above corona pressures was probably well sealed within the transformer windings.

The manufacturer had not considered it advisable to encapsulate the transformer windings because they felt that the differing thermal expansion coefficients of the encapsulant and the No. 44 copper wire in the secondary windings would cause difficulties and possible breakage, because of the broad temperature range which was specified for the operation of the supply.

5.6 SUMMARY

In the light of the information which has been described in this section we can put forward a theory which is substantiated by all the available data. Following launch of the instrument, the air trapped within the transformer element in the high voltage

power supply gradually leaked or diffused out of the module until its pressure reached a region favorable to corona breakdown between the leads or windings of the primary and secondary coils (see Figure 13). Then such breakdown occurred, yielding our "Mode I" condition and producing large transients on the common (return) line of the primary circuit, which were aggravated by the presence of the inductor and series resistor in that leg. These transients caused the capacitor C1 to open. As the corona breakdown condition continued, interaction with the materials of the transformer developed and reduced resistance paths, first intermittently and then more permanently, eventually producing the "Mode II" condition. Variation (with time) of the condition of these synthesized resistance paths produced the occasional reversion to Mode I observed on several later orbits. Clearly this is a theory, not a proven fact, although it is consistent with all the information available.

6.0 OTHER CONCURRENT ASPECTS

6.1 GENERAL

Immediately after the malfunction and for some time during the early analysis, additional pieces of data and suggestions became available concerning the instrument, spacecraft, or environment, which were thought to have some bearing on the malfunction. Each of these was reviewed carefully and in most cases discounted, either through careful study or because later data had become available. Some of the more important of these aspects will be discussed in detail here.

6.2 FLUCTUATIONS IN INSTRUMENT TEMPERATURE

Shortly after the malfunction, it was observed that the instrument's absolute temperature had risen from 17°C to 21°C in the period from November 25, through November 30. This was at the end of a long gradual rise in temperature (from 11°C) beginning in late October. In the eight days following the malfunction while the instrument power was off, the absolute temperature returned to 15°C and subsequently went even lower. How this related to the failure was uncertain. The instrument and its sub-assemblies had of course been acceptance tested over a much wider temperature range, in excess of 0°C through 30°C.

An analysis of the orbital characteristics, in particular the ratio of sunlight to darkness, for the period of interest was performed. The data were obtained from the NASA Predicted World Map and the results are

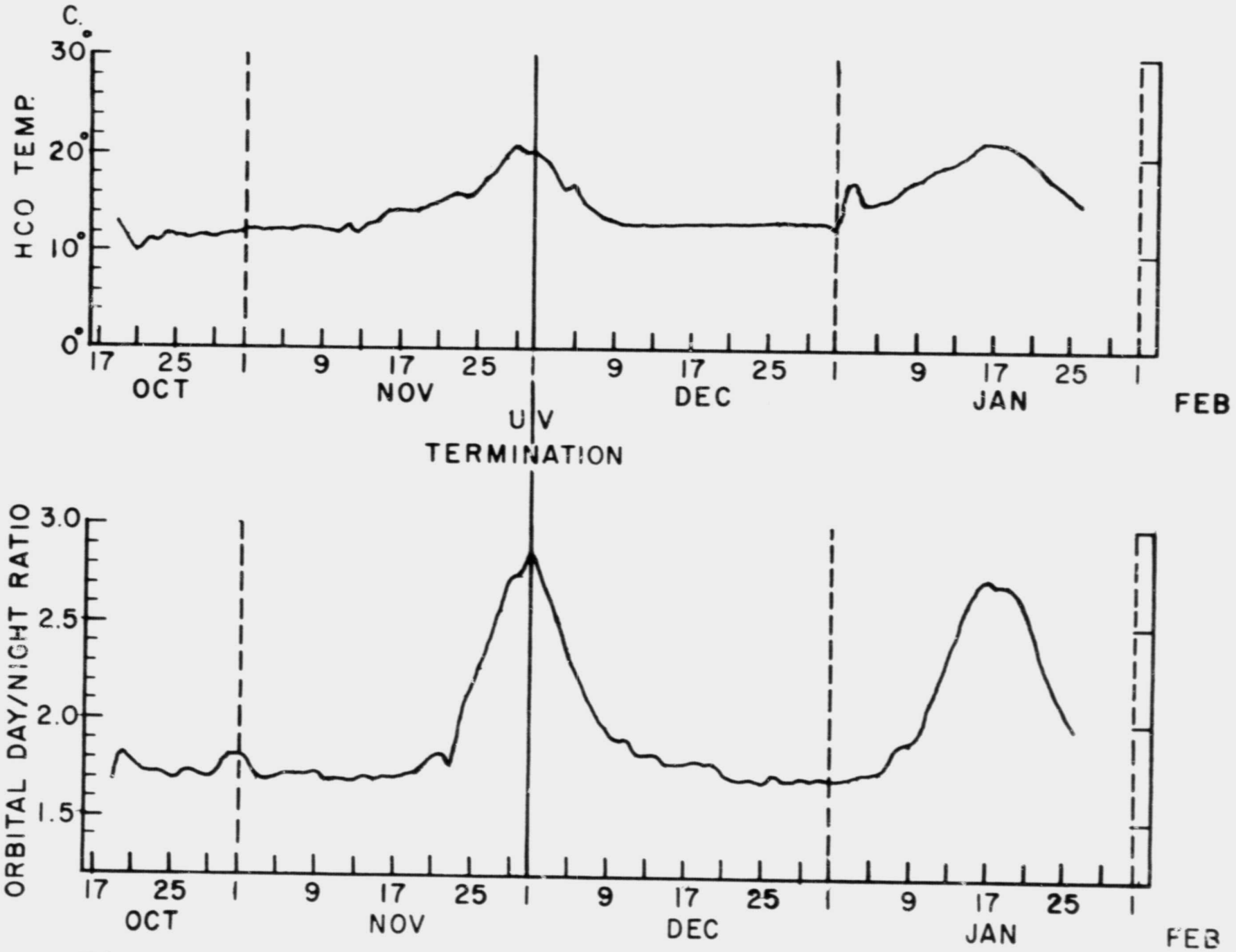

Figure 18 — OSO-Ⅳ ORBITAL CHARACTERISTICS

summarized in Figure 18. Fairly abrupt rises occur in this ratio periodically, because of the precession of the orbital plane at intervals of approximately 47 days. The instrument temperature appears to have followed these intervals faithfully. This was confirmed when the next peak occurred in mid-January and the instrument temperature performed a similar excursion. This effect has been noted on previous OSO's. Therefore the fluctuation in instrument temperature are believed to be a result of external causes rather than any pre-failure self-heating effect. However, it should be noted that the fluctuation in temperature might still have had a secondary relationship to the malfunction by altering the physical geometry of the gas leakage paths from the high voltage transformer by thermal expansion. A check of orbit 1238, in which a mode transition was observed, has shown that the thermal expansion occurred shortly before but not during one of these temperature excursions.

6.3 SOUTH ATLANTIC ANOMALY

As a result of HCO experimental difficulties on OSO-II and data from other experimenters, a substantial amount of study and testing had been performed on the HCO instrument for OSO-IV in order to avoid harmful effects on the instrument while passing through the South Atlantic Anomaly. Considerable testing of the plasma environment performed on the prototype model at the GSFC test facilities had convinced us that a modest but harmless effect on the data count would be observed.

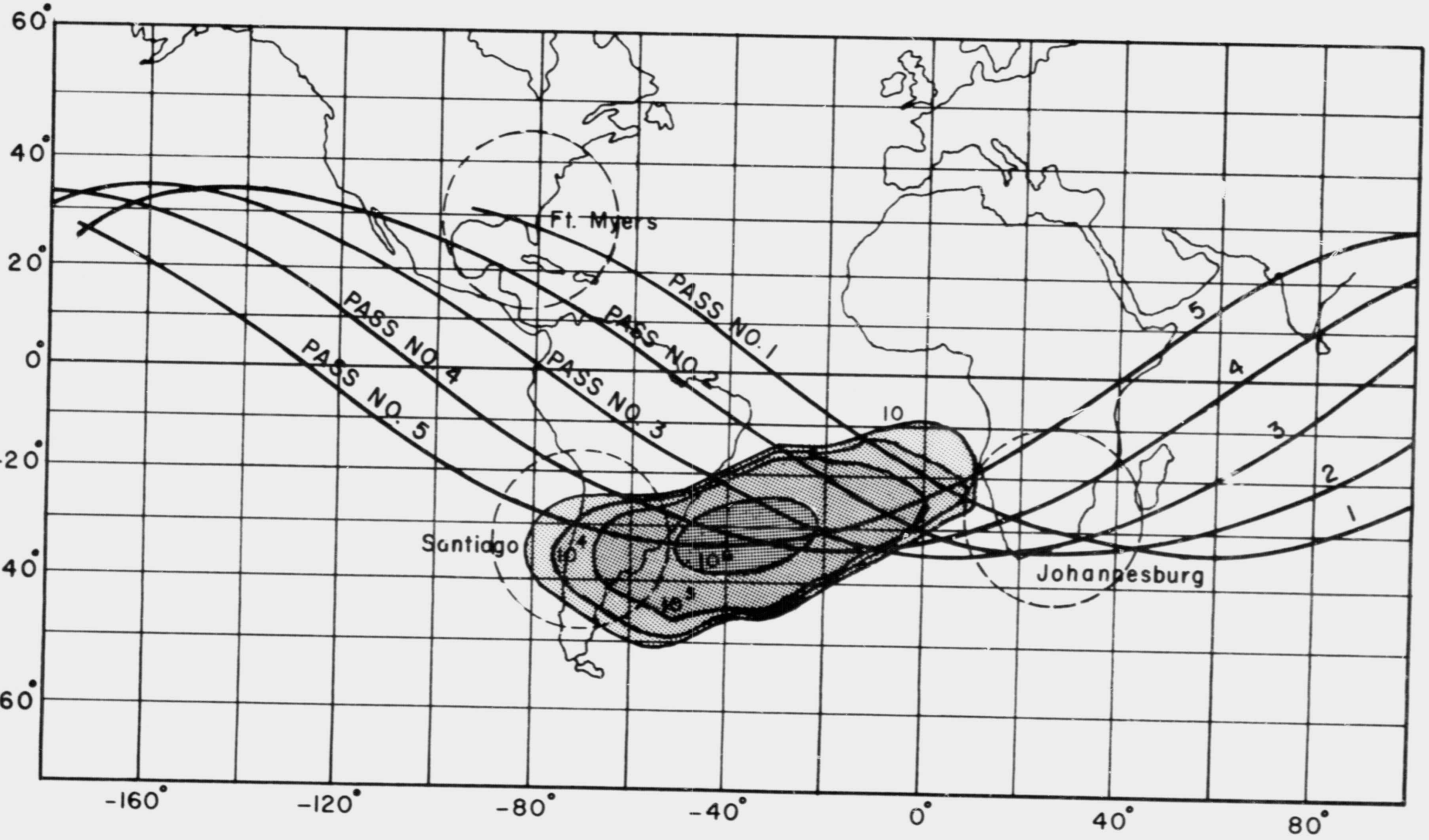

Figure 19– SOUTH ATLANTIC ANOMOLY

(Data Plotted by W. N. Hess, 3/14/66 – Omnidirectional Electron Flux – $E > .28$ Mev, 600 Km Altitude)

Approximately five to six of the fifteen daily orbits pass through the anomaly. As illustrated in Figure 19, the first of these contact with the anomaly occurred after the last daily pass over the Fort Myers STADAN Station. Thus the Fort Myers Station never received data which were recorded while the instrument was in the South Atlantic Anomaly. Because Fort Myers was the only station with which a Quick-Look data link had been established and we had not received any data from the other ground stations by the end of November, 1967, there was no occasion until the malfunction to observe any effects of the anomaly on the instrument. The data which we recovered especially from the Johannesburg Station after the failure, covered orbit 636 (equivalent to Orbit No. 1 in the illustration). These were the first data received that showed the interaction effects. Because it was the first observation, and made within the 30 minutes of failure, it caused some immediate concern. Later data analyses have discounted any immediate casual relationship to the failure.

A study of the data from all orbits was undertaken after the receipt of final data tapes in 1968. The data counts during a central pass through the anomaly ranged to 50 counts per integration time, although they averaged approximately 5 (60 counts per second). This was consistent over the many observations available.

The altitude of the pass through the anomaly seems to have had no appreciable effect. Data from the NASA

Predicted World Map shows that the altitude of the typical pass increased from approximately 560 kilometers in late October to a peak of 580 kilometers in early November, and then gradually descended to about 545 kilometers shortly before malfunction. No equivalent effect appears in the count data.

The extraction of the data relating to interaction with the anomaly was complicated by several factors. The data system was turned off during orbital night, and the effect is minor enough to be frequently masked by the UV signal in high intensity rasters or wavelength scan activities. Therefore, the data were obtained during very low intensity rasters, from the corner of raster patterns, and during the occasional situation in which the anomaly passage occurs at orbital sunrise or orbital sunset when the atmospheric absorption is high.

6.4 SPACECRAFT ANOMALIES

Two other anomalies have been raised for discussion as having possible significance in the malfunction analysis. On November 23, during orbit 544, the high voltage system of the experiment was found to be off, although the low voltage system remained on. This was not only unexpected but also highly unusual, in that the off command turns off both the high voltage and the low voltage. Therefore, either the high voltage power-on relay tripped out for reasons unknown, or two commands were received, namely to turn the instrument off and turn the low voltage system back on. Neither one

of these explanations is entirely satisfactory.

Another incident of interest was that about one week after the experiment malfunction, a number of synchronization losses were observed in the main frame and subcommutated data systems. These are usually associated with transients within the orbiting Observatory. A number of spurious commands were noted during this same period of time, particularly with the UCL Helium II experiment. Both effects disappeared when that experiment was deactivated.

Although both the effects noted above are probably associated with transients within the Observatory, and although they are not fully understood, they are in all probability not directly related to the HCO experiment failure.

6.5 SOLAR FLARES

There has been speculation that solar activity, and in particular the effects of solar flares, may have contributed to the instrument failure. A review of the available observations has shown that there were a considerable number of flares of a variety of classes and brightnesses during the five weeks prior to failure. Those of class 2 and 3 are listed in Table I. A number of these were actually observed in the UV data recovered by the experiment while scanning the solar disc in a raster pattern. The flares, however, vary considerably in their UV intensity and particle production, and in addition their classification is largely a qualitative matter.

Nonetheless, the conclusion can be drawn that particular flares were not a direct causative factor in this failure, for two reasons. First, no one flare, immediately prior to the malfunction was outstanding in its nature. Secondly, and more importantly, there was no observable effect in the instrument's telemetered data just before the failure (see Figure 5B). One would expect a high energy interaction to manifest itself in considerable noise in the data system, which was not observed.

The question as to whether there was a cumulative effect resulting from continuous exposure to the effects of solar activity will be difficult to establish because the quantitative measure of cumulative exposure is largely unknown, and in addition, the instrument's sensitivity is also unknown.

TABLE I

Part 1 Occurrence of Solar Flares*

DATE	QUANTITY	IMPORTANCE	UT
10/29/67	2	2B	0012
10/31	1	2B	1131
11/2	1	2B	0855
11/10	1	1B**	0852
11/16	1	3B	2143
	1	2B	2202
11/17	2	2B	0822
	1	2F	0835
11/29	1	2B	1200

Part 2 Principal Magnetic Storms

DATE	MAXIMAL ACTIVITY ON K-SCALE 0 TO 9	UT START	UT END MO	DA	HR
10/28/67	6-8	1637	10	30	10
11/3	5-6	08--	11	04	01
11/8	5-6	13--	11	08	24
11/29	3-5	0512	11	29	20

* (Selected examples)

** This single 1B Flare has been included because of the length of its duration.

7.0 CONCLUSIONS

The following conclusions can be drawn with reasonable confidence from the data available.

1. On November 29, 1967, an event occurred within the HCO OSO-IV pointed experiment which in a few seconds terminated UV data gathering, resulting in current limited operation of the high voltage power supply, and interaction with the primary data system of the instrument.
2. The event was an electrical interaction between the secondary and primary sections within the high voltage power supply, probably of moderately high resistance, and within the transformer section.
3. Shortly thereafter the capacitor C1 (within the HVPS) became open-circuited, probably from excessive voltage on the primary ground return, on the circuit side of the current monitoring resistor.
4. Intermittent transitions to another mode characterized by no noise in the data system and fluctuating excessive primary current occurred during the next 30 minutes, culminating in a more permanent transition to the second mode.
5. The second mode was a relatively stable low resistance path between the secondary section and the primary section of the high voltage power supply, probably within the transformer.

6. No reversion to a mode capable of gathering UV data has occurred since the first event.
7. The probable failure of the high voltage transformer is in all likelihood due to inadequate manufacturing and encapsulating technique. This resulted in trapping a significant pocket of air within the windings of the transformer, which gradually leaked out allowing eventual electrical breakdown.

8.0 RECOMMENDATIONS

Although this report does not attempt to be definitive on the measures which should be taken to minimize or eliminate the problems of handling high voltage in aerospace vehicles when considering the results of this experiment, certain areas stand out as needing further attention.

It should be pointed out that the malfunction of the HCO experiment was particularly disappointing in view of the measures taken during the design and testing of the instrument to minimize the problems and effects of high voltage. In addition to all the usual qualification and acceptance tests (including the thermal vacuum testing) the design was subjected to plasma environment testing at Goddard Space Flight Center in several configurations, and to spontaneous corona testing to evaluate its immunity to damage. If these tests showed areas of weakness, appropriate modules were redesigned and the tests repeated until no further problem occurred. Nonetheless, a failure occurred in orbit and the analysis has shown several areas needing further work. These fall generally into the categories of system design, detail design, and testing.

In the system design, two recommendations can be made. 1) High voltage failures, both in the laboratory and in this case in orbit, seem to be progressive affairs in which the continuation of one kind of effect precipitates another. A way of avoiding this chain of events is through the use of overload sensing devices

coupled with an automatic off switch. This technique will be used in our OSO-G experiment, and although it will not guarantee the avoidance of irreversible change, it should reduce the probability of it. Another technique to be considered is the use of redundant high voltage power supplies or complete systems to extend the probable life of an experiment.

In the area of detail design, extreme care should be exercised in both the design and implementation of an encapsulation system for each particular application. This includes attention not only to technique but also to the hardware design for ease of encapsulation. A careful evaluation of the trade off between physical size and reliability is important. Smaller transformers, or components in general, are harder to encapsulate properly. Attention should be paid to the physical layout of the high voltage system to avoid inadvertent proximity of the high voltage and ground systems. Another specific correction to be made in a new experiment is the addition of a capacitor (AC ground) between the primary return and ground. This would avoid the build up of high transients in the circuit.

The matter of testing needs further examination. This failure brings up a question of testing philosophy and whether flight units should be tested for relatively small proportions of their expected life or longer amounts. For example, typically a motor is subjected to tests equivalent to a small proportion of its expected life before flight. However, perhaps a high voltage power supply, for example, should be exposed to vacuum

for a period equivalent to its designed exposure time as a routine acceptance test. More generally the recommendation here is to thoughtfully design test procedures which completely explore as many areas of weakness as possible.

BIBLIOGRAPHY

1. Harvard College Observatory OSO-D Experiment Handbook, May 1, 1966, Harvard College Observatory, Cambridge, Massachusetts.

2. OSO-D Instrument Analog Channels Calibration Curves (unpublished - available at Harvard College Observatory, Solar Satellite Project, Cambridge, Massachusetts).

3. OSO Spacecraft Manual, July, 1966, (X-440-66-346), NASA, Goddard Space Flight Center, Greenbelt, Maryland.

4. Experimenter's Manual for the OSO, February, 1965, (X-623-65-73), NASA, Goddard Space Flight Center, Greenbelt, Maryland.

5. Experimenter's Manual for the OSO, Supplement #1, June, 1965, (X-623-65-73), NASA, Goddard Space Flight Center, Greenbelt, Maryland.

6. OSO-D Experiment Payload Description, (TN65-218, Revision A), February 1, 1967 Ball Brothers Research Corporation, Boulder, Colorado.

7. OSO-D Subcommutator Data Conversion Tables, (TN65-169, Revision B), September 23, 1966, Ball Brothers Research Corporation, Boulder, Colorado.

APPENDIX 1

DATA FORMAT

1.0 PCM DATA SYSTEM

Data from the HCO instrument is multiplexed into the main frame of the spacecraft's PCM data system as shown in Figure A-1. The spacecraft has an internal clock which generates a square wave of 400 cycles per second (cps). The timing of this clock sets the rate at which data readout from the various experiments is recorded on the spacecraft's taperecorder.

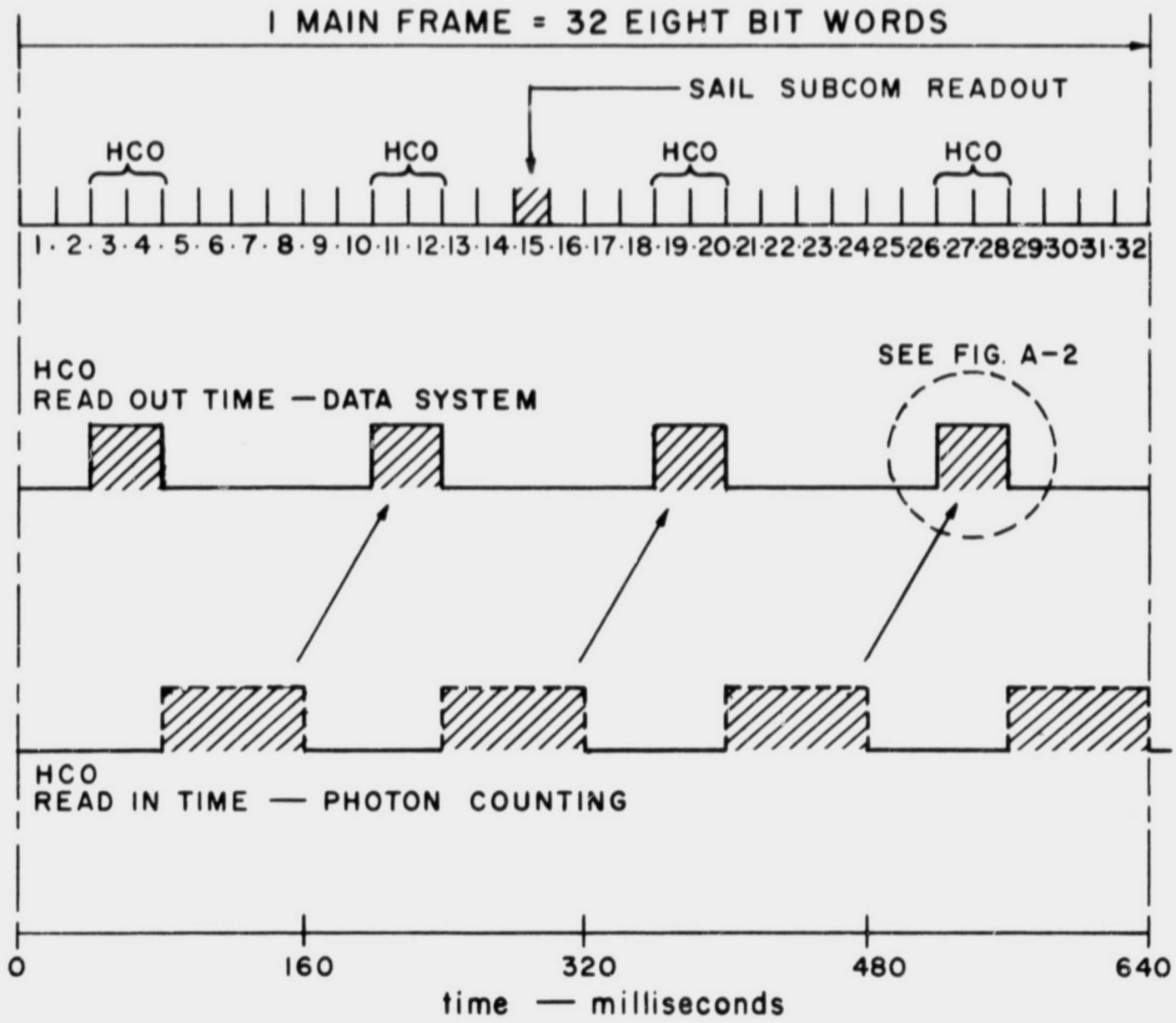

Figure A-1
HCO WORDS AND TIMING IN SPACECRAFT DATA SYSTEM

2.0 HARVARD WORDS IN SPACECRAFT'S MAIN DATA FRAME

During 20 milliseconds (ms) 8 binary bits of data are readout (8=20ms x 400 cps). Harvard has 40 ms of readout time for each of its four words in a main frame of data. Thus, each word is represented by 16 binary bits as shown in Figure A-2. Fourteen bits represent the state of the counter after the 80 ms read-in period during which current pulses produced by UV photons' incidents on the photomultiplier are counted. The last two bits are reference or flag bits that indicate the position of the diffraction grating.

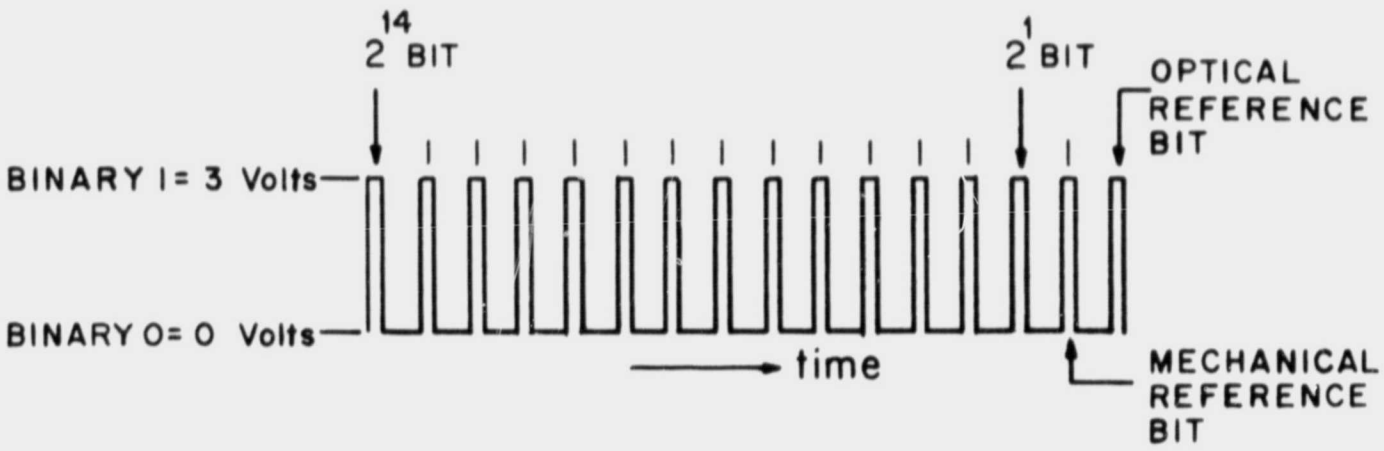

Figure A-2
HCO BINARY DATA WORD FORMAT

An "0" in the Mechanical Reference (MR) bit indicates:

i) the diffraction grating is in the MR position

ii) the instrument has completed a raster (this occurs in four successive words at the end of each raster)

iii) the instrument is in the night portion of its orbit

iv) the instrument is OFF (low voltage and high voltage power supplies turned off).

A "1" in the MR bit indicates the absence of the above conditions. A "1" in the Optical Reference (OR) bit indicates that the grating is in the OR position or in Retrace OR. A "0" in the OR bit indicates that the grating is in neither of those positions. Table A-I presents the translation from data reference bits to the All Channel (AC) computer printout format.

Table A-I

REFERENCE BIT STATES

Instrument Condition	Binary Data Bits MR bit OR bit	AC Printout Symbol
Grating in MR position or Night or End of raster or Instrument OFF	00	A
Grating in OR position or Grating in Retrace	11	D
Normal operating state (neither MR nor OR)	10	C
Forbidden state under normal conditions	01	B

In addition to its UV data word allocation in the spacecraft's data main frame, Harvard has six of the

forty-eight channels in the Sail Analog Subcommutator (ASC No. 2). These channels as listed in Table A-II are used to monitor internal instrument parameters.

Table A-II

HCO ANALOG CHANNELS

HCO Channel 1 (ASC No. 2-15)	Absolute Temperature. Indicates internal temperature at center of instrument. Normally ~20°C. (114 digitized)
HCO Channel 2 (ASC No. 2-21)	ΔT. Indicates difference in temperature between fore and aft ends of instrument. Normally varies once per orbit ~2-6°C. (136-217 digitized)
HCO Channel 3 (ASC No. 2-25)	High Voltage Current. Indicates current through the primary side of the HV power supply. Normally ~9 milliamperes. (35 digitized)
HCO Channel 4 (ASC No. 2-26)	Grating Position. Linear-potentiometer indicates position of diffraction grating from retrace (190 digitized) to 0 steps (Mech. Ref.) (50 digitized) Linipot summed with -3V supply voltage. -3V failure biases output 1 volt positive.
HCO Channel 5 (ASC No. 2-30)	Sums -5.5V Supply voltage with integrated Read-In Gate waveform. Normally +1.1V (55 digitized).
HCO Channel 6 (ASC No. 2-43)	Sums +4.2V Supply voltage with Pulse Amp Output. With no counts analog signal is +4.2V (213 digitized). Analog signal decreases with increase in Pulse Amp Output frequency.

Analog readings are provided by transducers and special circuit arrangements within the instrument. These yield analog voltages from 0 to 5 volts under normal conditions. The Sail analog voltages are sampled and encoded during 160 microseconds (μsec.) at the beginning of word 15 in the data main frame. The digital multiplexer and encoder converts an analog voltage to an eight bit binary word by a method of successive approximation: the most significant bit (2^7 bit) is encoded first during 20 μ sec., then the next most significant bit (2^6 bit) during the following 20 μ sec., and so on to the least significant bit (2^0 bit) during the final 20 μ sec. of the 160 μ sec. sampling and encoding time. The encoding is designed to be linear with a range of 0 to 255 counts (see Figure A-3).

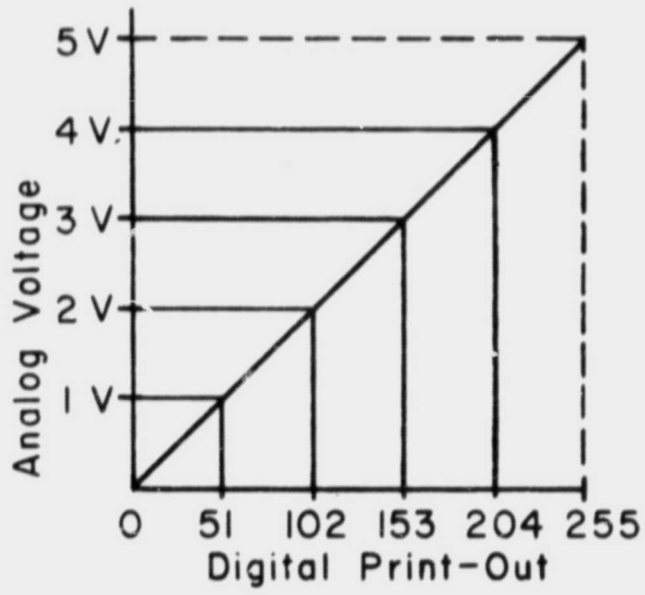

Figure A-3
ANALOG-DIGITAL CONVERSION

One Sail Subcommutator channel is read out during word 15 of each data main frame (MF). The readout begins

just after the sampling and encoding time. The 48 Subcommutator channels are read out during 48 successive main frames. Thus, any one Analog Channel is read out once every 30.72 seconds (30.72 sec. = 48 MF x 0.64 sec/MF) under normal operating conditions.

APPENDIX II

CORONA AND HIGH VOLTAGE BREAKDOWN OF ELECTRICAL CONDUCTORS IN VACUUM*

1.0 INTRODUCTION

Corona is defined as an electrical discharge caused by ionization of the gas in the vicinity of a conductor. This ionization can occur on the surface of an insulated or uninsulated conductor as well as in voids and cracks within the electric insulation. To produce corona, a voltage gradient must exist along the conductor, or between the conductor and some other nearby conductor. To implement effective design practices which will minimize the possible detrimental effects of high voltage, the phenomena of electric corona and breakdown must first be understood.

This report presents a brief description of corona and some of the technique to prevent its occurrence.

2.0 DISCUSSION

If an electric field is applied across a solid insulator and a gas, as shown in Figure A-4 the gas will normally break down by ionization and conduct at an applied voltage much less than that required to rupture the insulator.

---

* The material in this appendix is adapted from Appendix E of Experimenter's Manual for the OSO, Supplement #1. It was prepared by the Failure Analysis Section, Quality Assurance Branch, Test and Evaluation Division of the GSFC Office of Technical Services.

There are two reasons for this.

1. At standard temperature and pressure, the gas has a lower dielectric strength, on a volts-per-mil basis, than the insulation.

2. The distribution of the electric field within the gas and the insulation is inversely proportional to the dielectric constants of the gas and the insulation (as discussed in Note 1).

When the stress on the gas, near the surface of a solid insulator or in a void in the insulator, exceeds the breakdown or ionization level, the gas becomes conductive and a pulse of current passes through the gas-filled space. Since the insulator does not conduct, the current passing through the gas terminates at the insulator and charges the surface. This charge produces a field that opposes the applied field and rapidly extinguishes the corona discharge. If the applied voltage is from a constant potential source, another discharge will not occur until the first charge has leaked off. An alternating voltage, however, will continuously change the field across the gap and produce a series of corona breakdowns, each of which will be generally less than 0.1 microsecond in duration. This intermittent characteristic distinguishes corona from continuous electrical discharges, such as electric arcs. It has also been determined that the corona starting voltage is independent of the applied frequency over the range from 6 cps to about 1 Mc.

3.0 EFFECTS OF CORONA ON INSULATORS

The energetic particles created when the gas ionizes are attracted toward and bombard the insulator, producing pits and cavities by slowly eroding away the surface. After a reasonably long period, depending on the corona intensity, excessive erosion will cause the insulator to break down.

The insulator breakdown can also occur when only a small amount of insulation is eroded away. In such cases, a recently-recognized phenomenon, known as "treeing", may be found penetrating the uneroded insulation, as shown in Figure A-4. Treeing is a progressive failure in which bracking occurs, hollow channels slowly penetrate through the insulation at applied voltage stresses of 50 volts/mil or less. This occurs because the electrical stress at the ends of the channels is so concentrated that the intrinsic insulation strength is locally exceeded. It has been observed that trees will grow at lower peak alternating voltages than constant voltages, the probable reason being that pulses and transients encourage propagation. Although the mechanism of propagation is not completely understood, it is believed that the current is carried within the channels by a succession of corona discharges.

Corona discharge in air also forms ozone and oxides of nitrogen which often react with the insulator and surrounding materials to produce undesirable nitrates and other compounds. An example of the detrimental effect of these reactions is the degradation of polyethylene insulation through the formation of a surface residue of oxalic acid.

4.0 EFFECTS OF VACUUM ON CORONA

Corona and insulation breakdown problems are magnified by the changing environment experienced by spacecraft traveling from normal sea level pressure to the hard vacuum of outer space. There is a pressure level roughly corresponding to an altitude of 20 to 50 miles, where corona and breakdown problems seem to be maximized. This problem area is explained by Paschen's Law which states that the breakdown voltage between two electrodes is a function of the product of the absolute pressure (p) and the spacing of the electrodes (d). It further states that the breakdown voltage decreases gradually with the pd product, down to a certain minimum, after which it rises again rather abruptly as the product pd decreases further. This minimum for air is approximately 330 volts and corresponds to a product of 5.8 (mm Hg x mm). Paschen's Law curves for oxygen, air and hydrogen are shown in Figure A-5. The exact shape, location and minimum of these curves depend upon: 1) the shape of the electrodes, 2) the electrode material, 3) the nature of the gas between the electrodes.

The Paschen's Law minimum can be explained by the association between the mean-free-path of the residual gas atoms and the energy necessary for the ionization of these atoms. Above Paschen's minimum, where gas pressure and density are relatively high, the atomic mean-free-path is short, resulting in multiple elastic collisions and little gas ionization. In the vicinity of Paschen's minimum, the atomic mean-free-path optimizes ionization with respect to the applied voltage.

As the pressure is further reduced, the atomic mean-free-path becomes so great that an insufficient number of ionizing collisions can occur.

It can be seen from Figure A-5 that, under certain conditions of pressure and electrode spacing, corona can occur at applied voltages as low as 327 volts in air. The nature of the residual gas environment has a major effect on this minimum. Oxygen, for example, has a Paschen's minimum of 440 volts and hydrogen a minimum of 292 volts.

As previously mentioned, corona is a pulse phenomenon whose duration is generally less than 0.1 microsecond and whose repetition rate may be random. Short duration pulses of this type can radiate high frequency components well into the 100 Mc region. This random radiation can be a major source for interference for sensitive instruments and communications equipment, and should, therefore, be minimized or eliminated. Corona can also exist as a continuous series of pulses up to a frequency of about 200 kc. As can be seen in Figure A-6, corona frequency (pulse repetition rate) is a function of corona current and absolute pressure. In a series gas-solid insulation system, corona current is dependent upon insulation leakage resistance and is normally well below that necessary to maintain corona as a regular series of pulses. Below the minimum current and pressure shown in Figure A-6, corona becomes a diffuse, intermittent series of pulses.

Note 1

DEVELOPMENT OF RELATIONSHIP BETWEEN ELECTRIC FIELD AND DIELECTRIC CONSTANT

The relationship between electric field and dielectric constant can be demonstrated by reference to Figure A-4, which illustrates a conductor/insulator system where:

d_1 = thickness of insulator
d_2 = thickness of residual gas space
k_1 = dielectric constant of insulator
k_2 = dielectric constant of residual gas
V_1 = total electric field across insulator
V_2 = total electric field across residual gas space
V = total electric field (applied voltage) across conductor/insulator/residual gas space

Applying the fundamental formulae of parallel plate capacitors:

$$C = \frac{Q}{V} \text{ -- (1)} \qquad C = \frac{kA}{d} \text{ -- (2)}$$

where:

Q = charge (coulombs)
V = voltage (volts)
C = capacitance (farads)
k = dielectric constant
A = area of one plate (sq. cm.)
d = distance between plates (cm.)

we find that:

$$V = \frac{Qd}{kA} \text{ -- (3)}$$

Applying (3) to the conductor/insulator system and assuming that the charge (Q) and area (A) is the same throughout the system, we find that:

$$V_1 \alpha \frac{d_1}{kA} \text{ and } V_2 \; 2 \; \frac{d_2}{k_2}$$

This demonstrates that the electric field across either the residual gas space or the insulation is:

(a) inversely proportional to the dielectric constants (k_1 and k_2)

(b) directly proportional to the thickness (d_1 and d_2)

The total applied field V is then equal to the sum of the individual fields or:

$$V \alpha \frac{d_1}{k_1} + \frac{d_2}{k_2}$$

Gasses by nature possess dielectric constants that are lower than those of liquids or solids. The dielectric constants of some materials typically used as insulator are listed below.

Vacuum, Dry Air, Nitrogen, Oxygen	1.0
Polystyrene	2.5
Polytetrafluoroethylene (Teflon)	2.0
Polyethylene Terephthalate (Mylar)	3.0
Mica	6.8
Ceramic (magnesium, titanate) up to	20.0
Ceramic (titania)	80.0 to 100.0

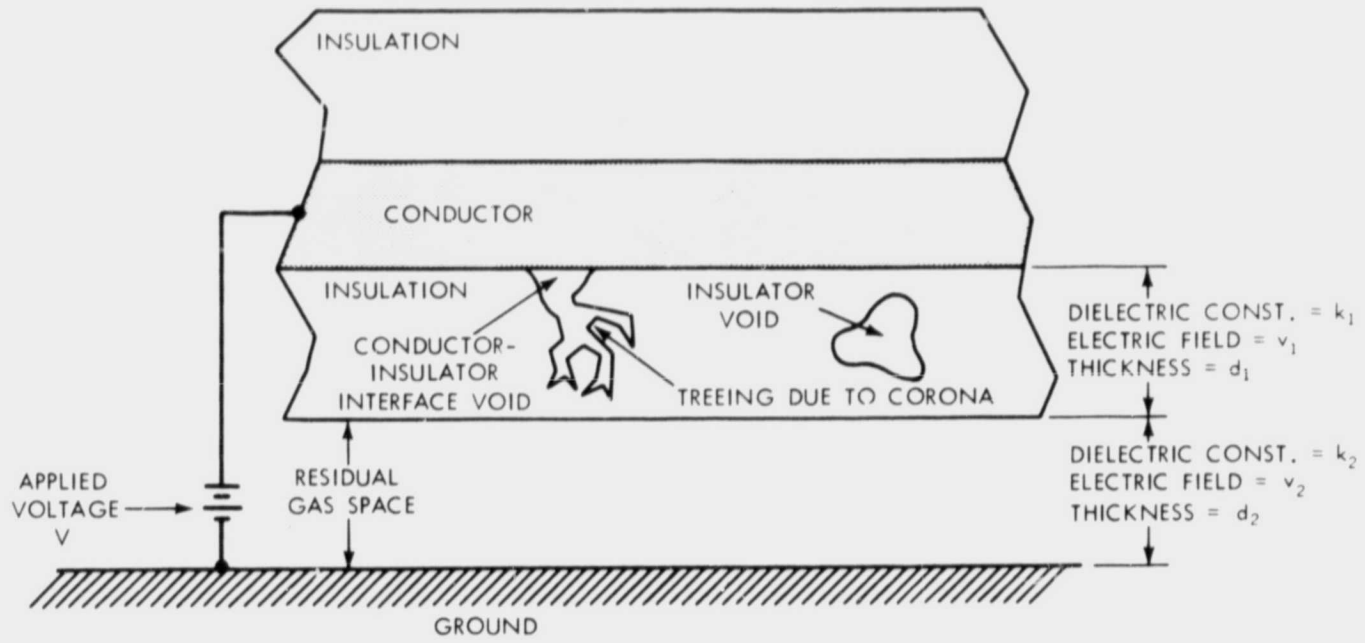

Figure A-4—Cross Section of Typical Conductor-Insulator System

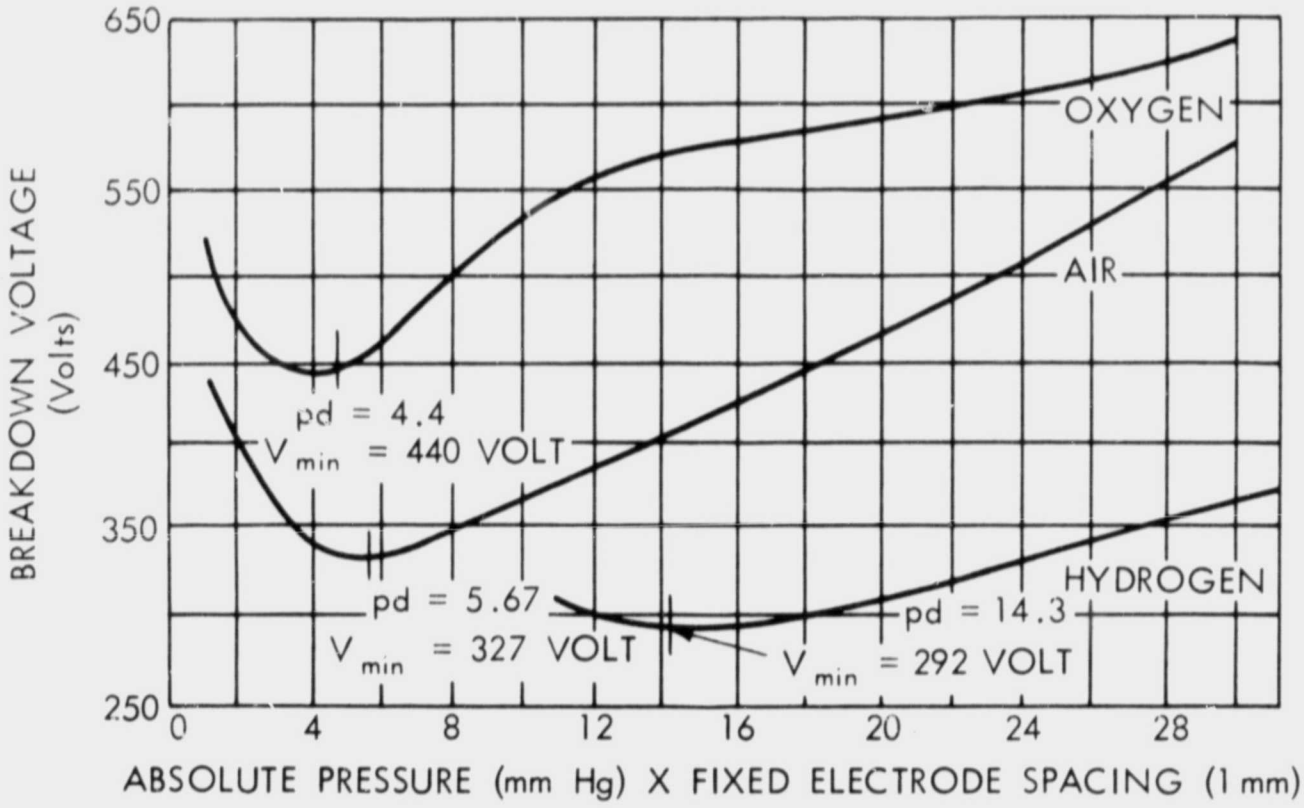

Figure A-5—Paschen's Law Curves for Oxygen, Air, and Hydrogen with Electrode Spacing Fixed at 1mm.

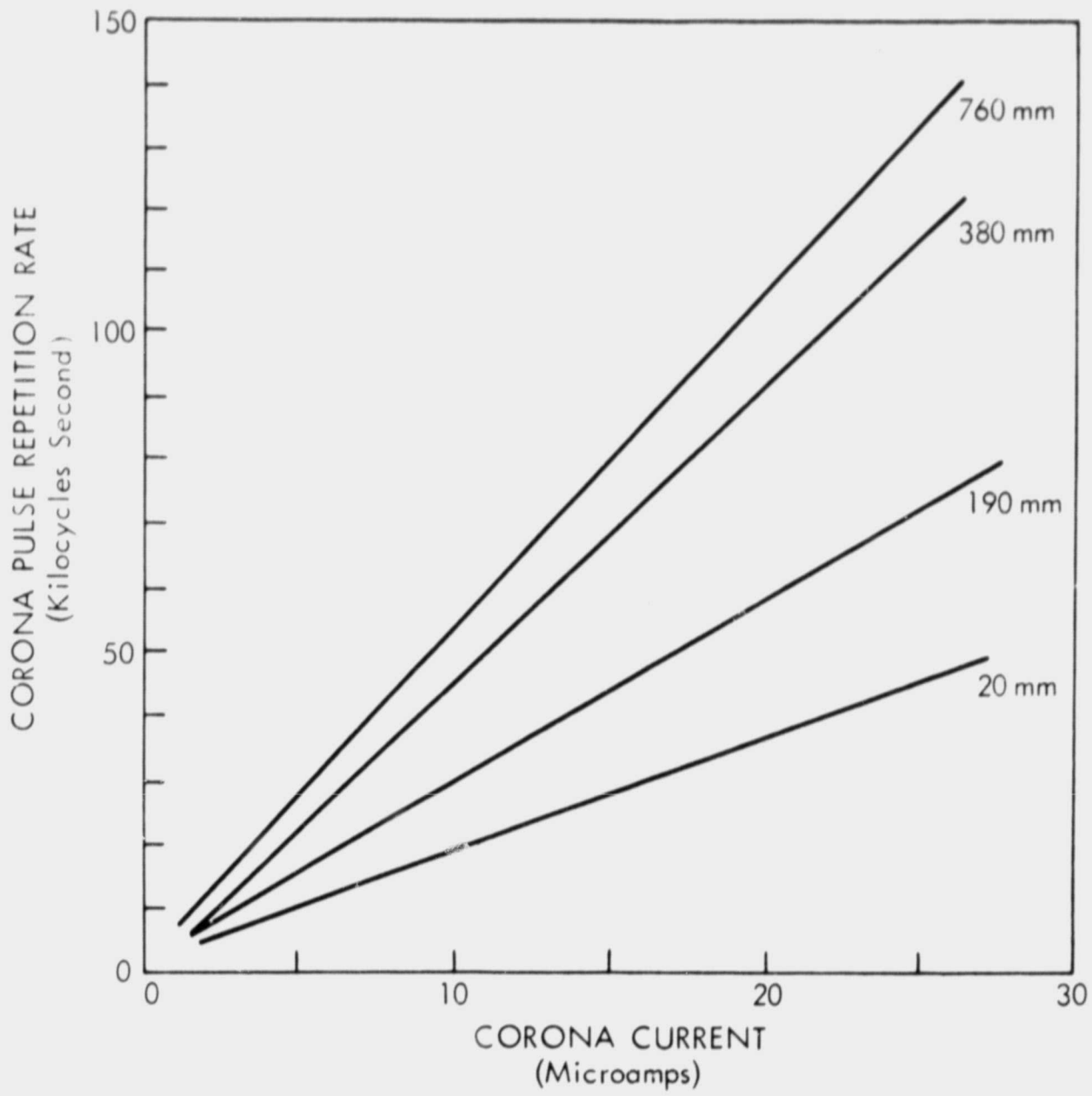

Figure A-6—Corona Pulse Repetition Rate as a Function of Corona Current and Absolute Pressure.